Supplementary Information

Physico-geometrical kinetic insight into multistep thermal dehydration of calcium hydrogen phosphate dihydrate

Masami Hara and Nobuyoshi Koga*

Chemistry Laboratory, Department of Science Education, Graduate School of Humanities and Social Sciences, 1-1-1 Kagamiyama, Higashi-Hiroshima 739-8524, Japan

Contents

* Corresponding author. E-mail: nkoga@hiroshima-u.ac.jp

S1. Sample Characterization

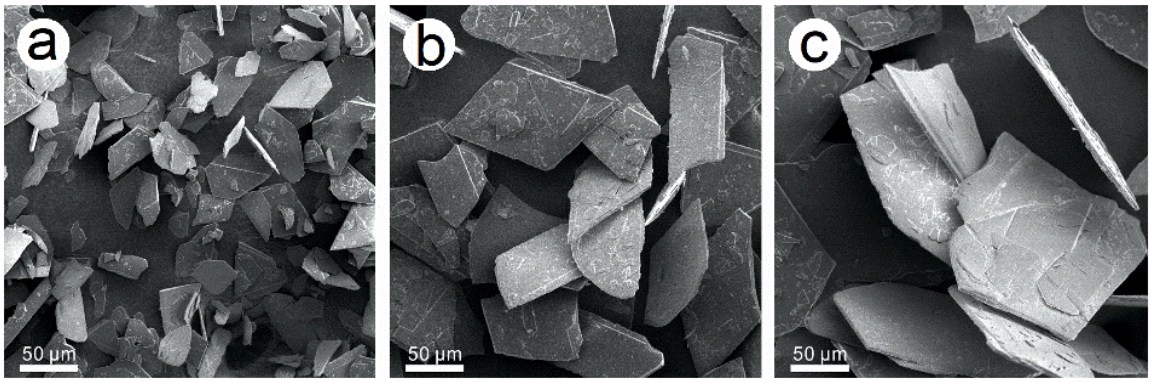

Figure S1. Appearances of sample particles in different particle size fractions: (a) 20–45, (b) 63–75, and (c) 90–150 μm.

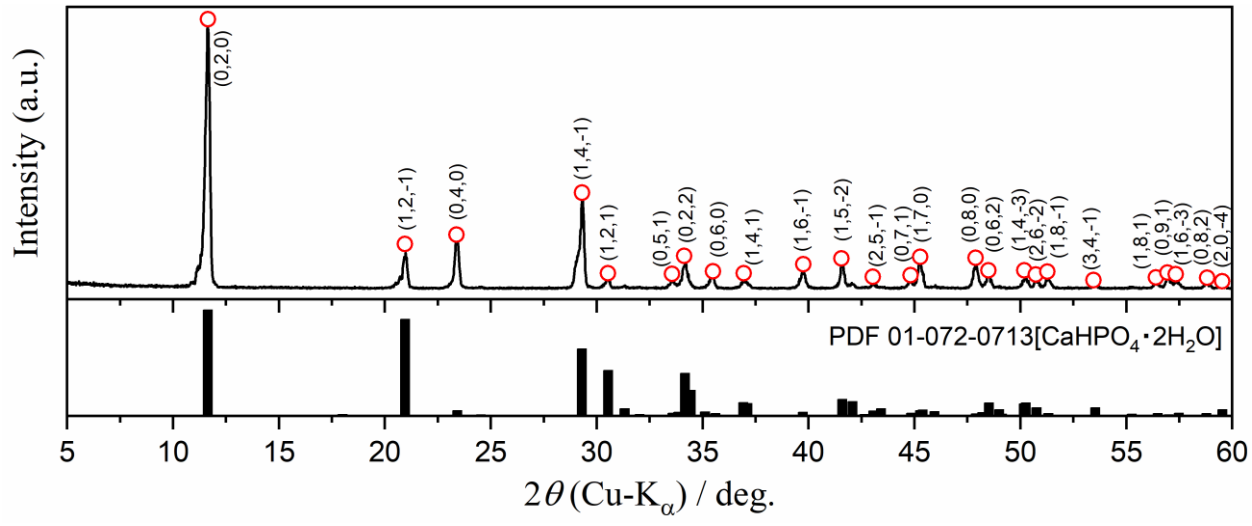

Figure S2. XRD pattern of DCPD.

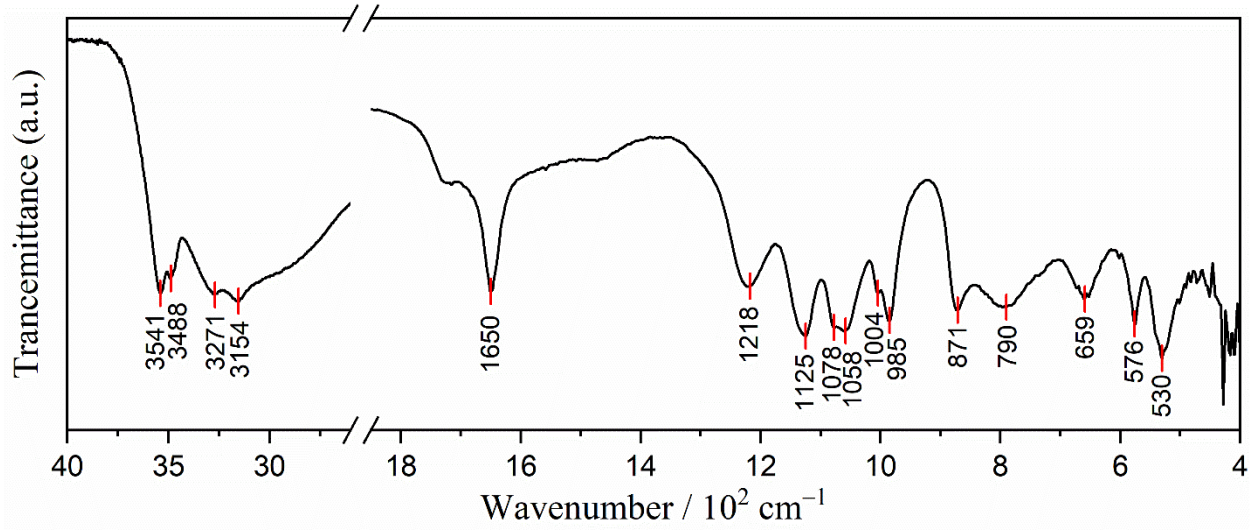

Figure S3. FTIR spectra of DCPD.

Table S1. Assignments of the IR absorption peaks of DCPD

Wave number/ cm^{-1}	Vibration mode
3541,3488 3271,3154	O–H stretching modes of water
1650	H_2O bending
1218	In-plane P–O–H bending
1125,1078 1058	P–O stretching modes
1004, 985	P–O symmetrical stretching modes
871	P–O(H) Stretching modes
790	Rotation of the O–H bond about the P–O(H)
659	Water vibration
576, 530	O–P–O(H) bending modes

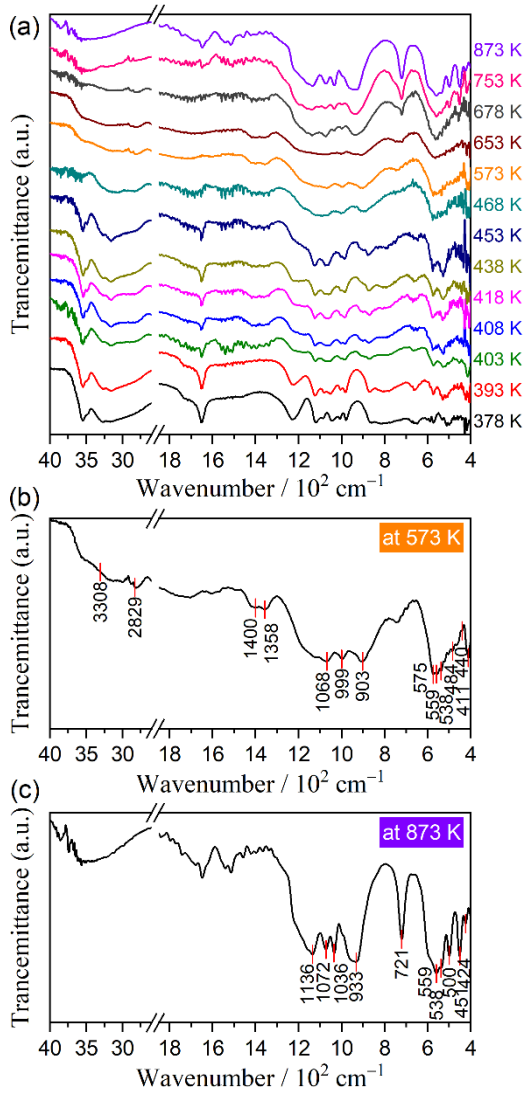

Figure S4. Change in the FTIR spectrum accompanied by the thermal dehydration of DCPD by heating to different temperatures at a β of 5 K min^{-1} in a stream of dry N_2: (a) FTIR spectrum at different temperatures, (b) FTIR spectra at 573 K, and (c) FTIR spectra at 873 K.

Table S2. Assignments of the IR absorption peaks of DCPA

Wave number / cm^{-1}	Vibration mode
3308, 2829	O–H stretching
1400	O–H in-plane bending
1358	In-plane P–O–H bending
1068	P–O stretching (ν_3)
999	P–O stretching (ν_1)
903	P–O(H) stretching
575, 559 538	P–O bending (ν_4)
484	combination
440, 411	P–O bending (ν_2)

Table S3. Assignments of the IR absorption peaks of γ-CPP

Wave number / cm^{-1}	Vibration mode
1136	Asymmetrical stretching of PO_3
1072	Symmetrical stretching of PO_3
1036	Asymmetrical stretching of PO_3
933	Asymmetrical stretching of P–O–P
721	Symmetrical stretching of P–O–P
559, 538 484, 440 411	PO_2 bending

S2. Multistep Thermal Dehydration of DCPD in a Stream of Dry N_2

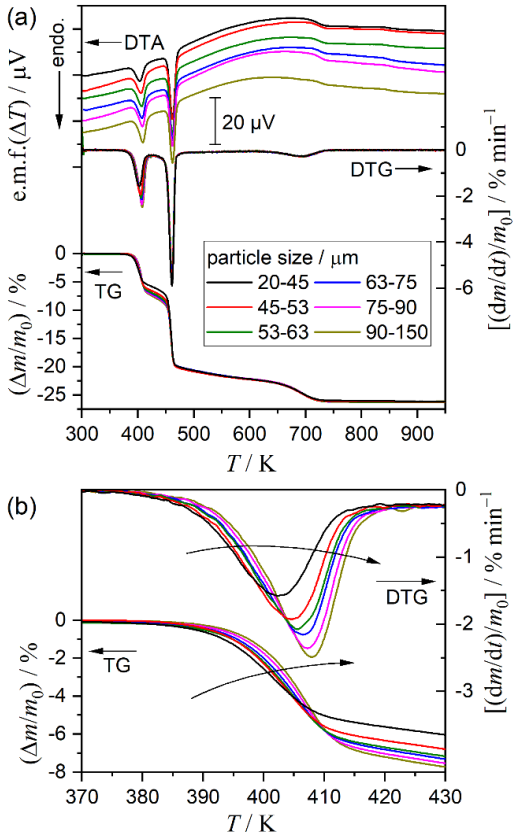

Figure S5. TG–DTG–DTA curves for the thermal dehydration of DCPD (m_0 = 5.00 ± 0.03 mg) with different particle sizes recorded at a β of 5 K min^{-1} in a stream of dry N_2 (q_v = 300 cm^3 min^{-1}): (a) overall view and (b) focused on the first mass loss step.

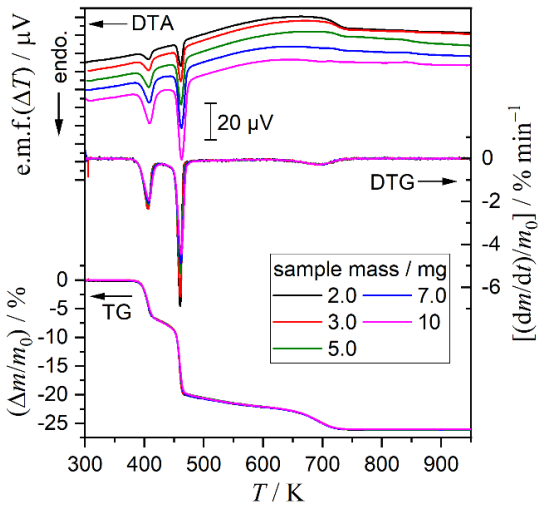

Figure S6. TG–DTG–DTA curves for the thermal dehydration of DCPD (63–75 μm) with different m_0 values at a β of 5 K min^{-1} in a stream of dry N_2 (q_v = 300 cm^3 min^{-1}).

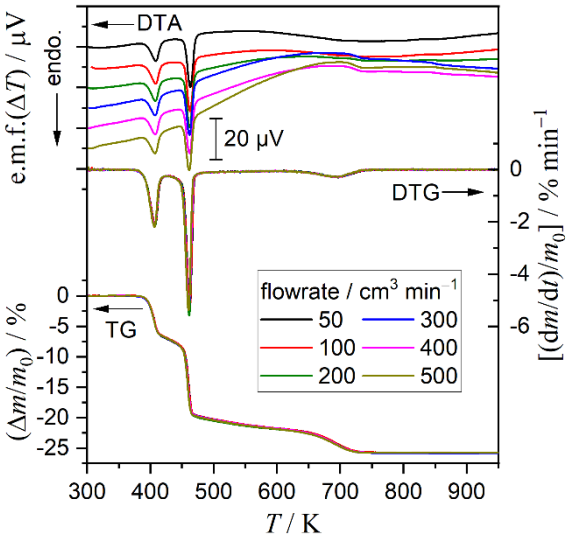

Figure S7. TG–DTG–DTA curves for the thermal dehydration of DCPD (63–75 μm; m_0 = 5.00 ± 0.03 mg) at a β of 5 K min^{-1} in a stream of dry N_2 at different q_v values.

S3. Mathematical Deconvolution Analysis for the Thermal Dehydration in a Stream of Dry N_2

MDA was performed for the DTG curves of the overall process under linear nonisothermal conditions by applying log-normal 4-parameter function:

$$F(t) = a_0 \exp\left[-\frac{\ln(2)\ln\left(\frac{(t-a_1)({a_3}^2-1)}{a_2 a_3}+1\right)^2}{\ln(a_3)^2}\right] \quad \text{(S1)}$$

where a_0, a_1, a_2, and a_3 are amplitude, center, width, and shape, respectively.

Figure S8 shows the typical fitting results of MDA. Irrespective of β, fitting using the log-normal 4-parameter functions applied to individual mass loss steps were nearly perfect exhibiting the determination coefficient (R^2) better than 0.99 (Figure S8(a)). The contributions (c_i) of each step i evaluated from the area ratio of the separated DTG peaks at each β value exhibited systematic increase in the c_i values for the first and second steps and accompanied decrease in that of the third step (Figure S8(b)).

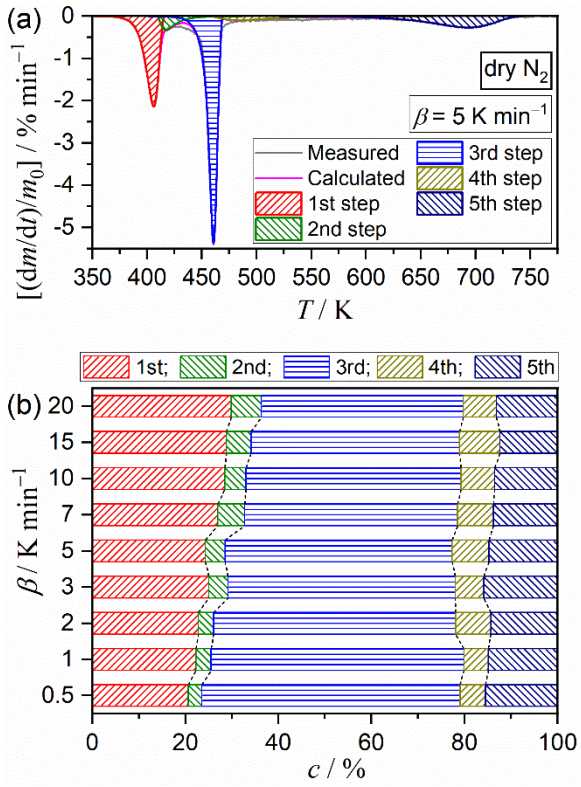

Figure S8. Result of MDA for the multistep thermal dehydration of DCPD (63–75 μm) in a stream of dry N_2: (a) typical fitting results for the overall reaction under linear nonisothermal conditions at a β of 5 K min^{-1} and (b) contributions of individual steps at various β values.

The kinetic curves of individual step at different β values were obtained from the separated DTG peaks by calculating the degree of reaction for each reaction step (α_i) with reference to the total area of the separated DTG peak, as shown in Figure S9. The kinetic curves of individual steps were subjected to Friedman plots (Figure S10). The $E_{a,i}$ values at different α_i determined by the Friedman plot exhibited nearly constant values for individual steps except fourth step (Figure S11). Using the $E_{a,i}$ values average over $0.1 \leq \alpha_i \leq 0.9$, the hypothetical reaction rate ($d\alpha_i/d\theta_i$) at an infinite temperature at different α_i values were calculated based on Ozawa's generalized time (θ) concept.

$$\frac{d\alpha}{d\theta} = \left(\frac{d\alpha}{dt}\right)\exp\left(\frac{E_a}{RT}\right) = Af(\alpha)$$

$$\text{with} \qquad \theta = \int_0^t \exp\left(-\frac{E_a}{RT}\right)dt \qquad \text{(S2)}$$

Accordingly, experimental master plots of ($d\alpha_i/d\theta_i$) versus α_i were created for individual steps (Figure S12). The experimental master plots were fitted using SB(m_i, n_i, p_i) function according to eq. (S2), and the A_i value and the kinetic exponents in SB(m_i, n_i, p_i) were optimized for each step. The kinetic parameters obtained by the isoconversional analysis and subsequent mater plot method were summarized in Table S4. These kinetic parameters listed in Table S4 and illustrated in Figure S8(b) were used as the initial values for KDA.

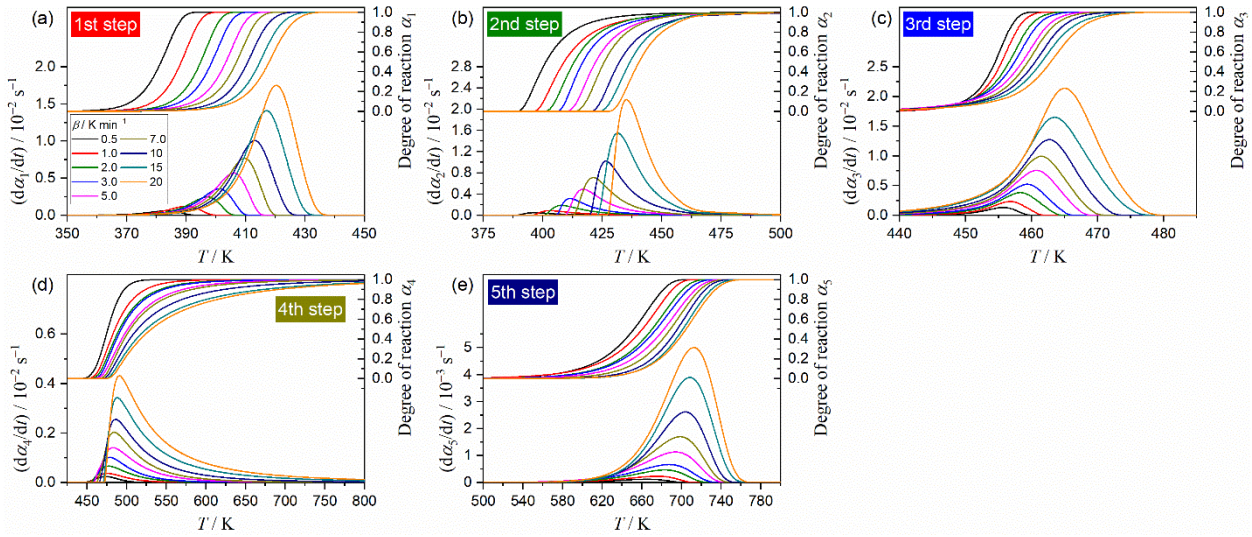

Figure S9. Kinetic curves for each reaction step of the multistep thermal dehydration of DCPD (63–75 μm) in a stream of dry N_2: (a) first, (b) second, (c) third, (d) fourth, and (e) fifth steps.

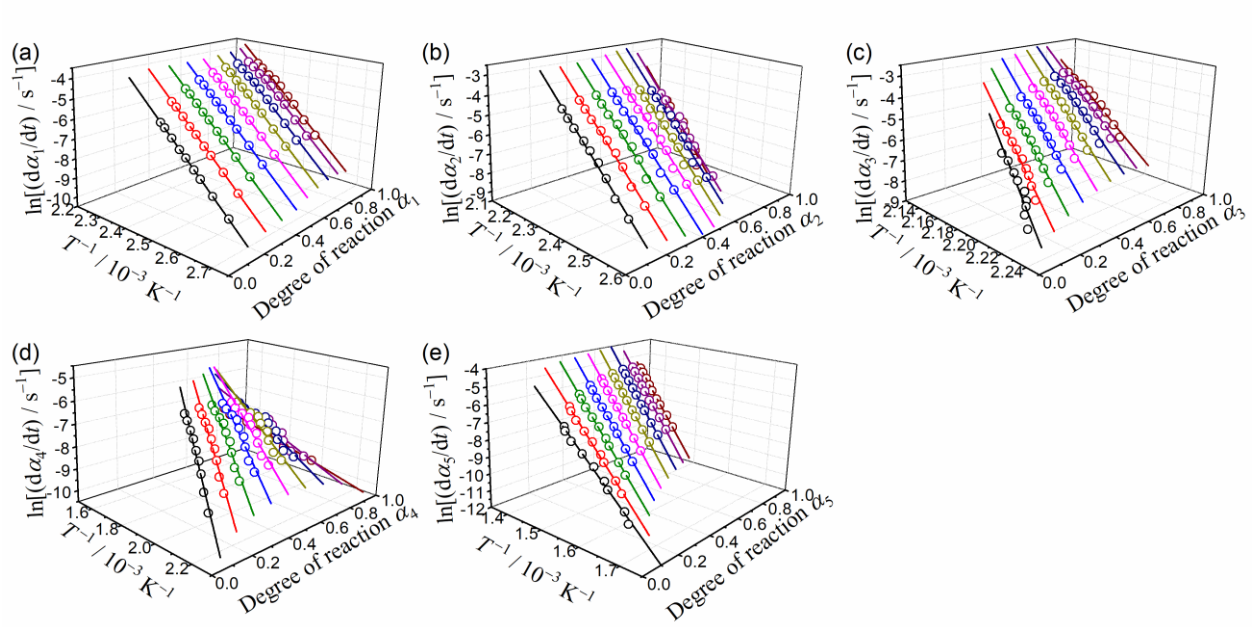

Figure S10. Friedman plots for each step of the multistep thermal dehydration of DCPD (63–75 μm) in a stream of dry N_2: (a) first, (b) second, (c) third, (d) fourth, and (e) fifth steps.

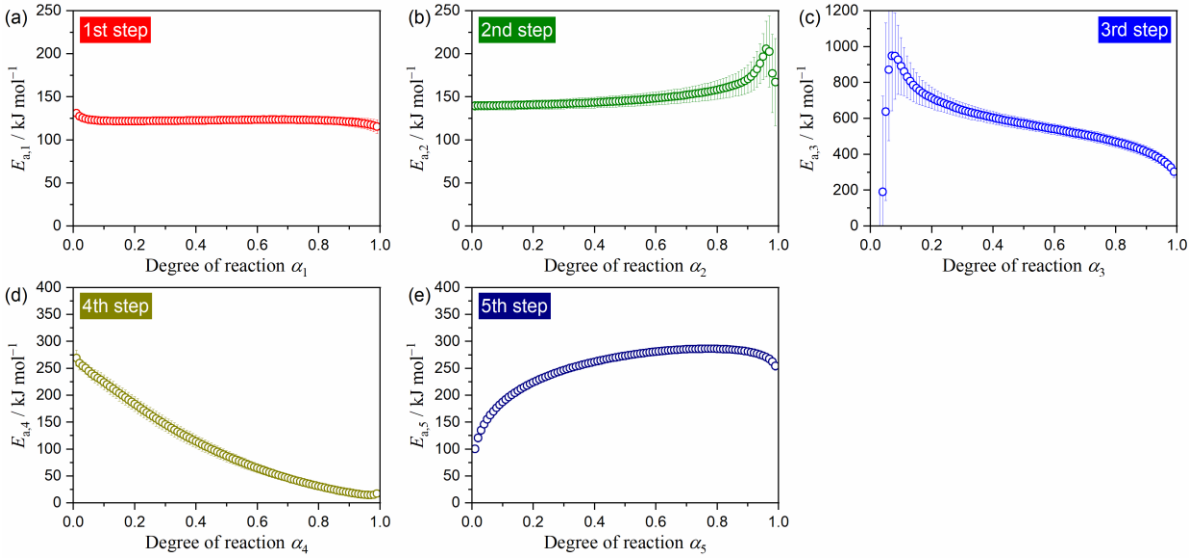

Figure S11. $E_{a,i}$ values at various α_i values determined by the Friedman plots applied to the mathematically separated kinetic curves: (a) first, (b) second, (c) third, (d) fourth, and (e) fifth steps.

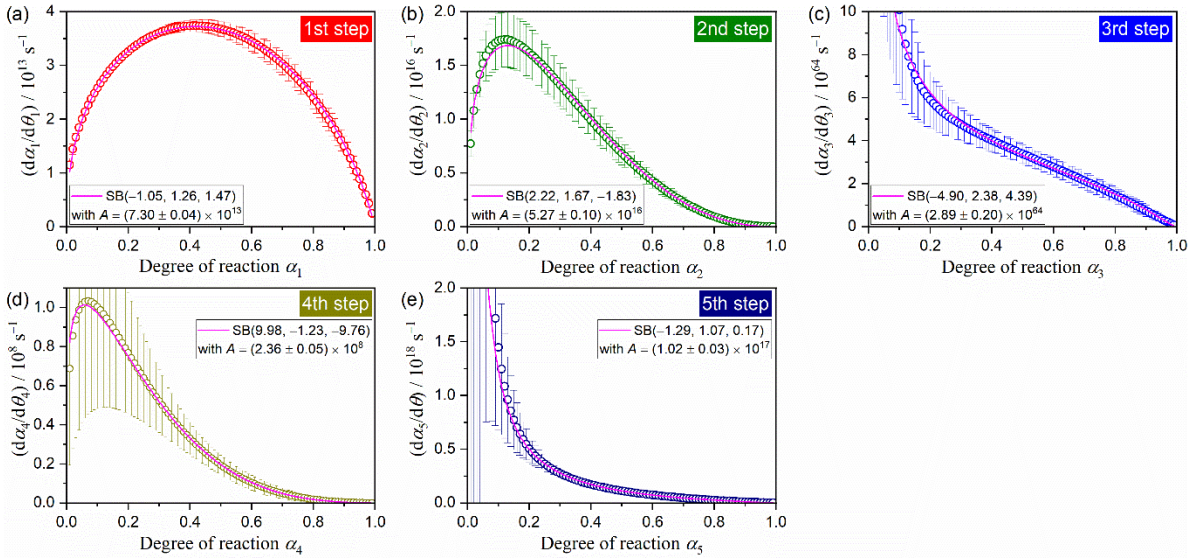

Figure S12. Experimental master plots for each step of the multistep thermal dehydration of DCPD in a stream of dry N_2: (a) first, (b) second, (c) third, (d) fourth, and (e) fifth steps.

Table S4. Results of mathematical deconvolution analysis and subsequent formal kinetic analysis for the multistep thermal dehydration of DCPD (63–75 μm) in a stream of dry N_2

i	$E_{a,i}$/ kJ mol^{-1}, [a]	$\frac{d\alpha_i}{d\theta_i} = A_i f(\alpha_i)$ with $f(\alpha_i) = \alpha_i^{m_i}(1-\alpha_i)^{n_i}[-\ln(1-\alpha_i)]^{p_i}$				
		A_i / s^{-1}	m_i	n_i	p_i	R^{2}, [b]
1	122.6 ± 0.7	(7.30 ± 0.04) × 10^{13}	−1.05 ± 0.08	1.26 ± 0.04	1.47 ± 0.08	0.9995
2	148.0 ± 7.8	(5.27 ± 0.10) × 10^{16}	2.22 ± 0.20	1.67 ± 0.08	–1.83 ± 0.19	0.9992
3	586.2 ± 107.2	(2.89 ± 0.20) × 10^{64}	−4.90 ± 0.60	2.38 ± 0.22	4.39 ± 0.57	0.9961
4	99.2 ± 60.7	(2.36 ± 0.05) × 10^{8}	9.98 ± 0.25	–1.23 ± 0.10	–9.76 ± 0.24	0.9995
5	261.8 ± 27.4	(1.02 ± 0.03) × 10^{17}	–1.29 ± 0.13	1.07 ± 0.04	0.17 ± 0.11	0.9997

[a]Average value over $0.1 \le \alpha \le 0.9$.
[b]Determination coefficient of the nonlinear least-squares analysis for fitting the experimental master plot.

S4. Kinetic Analysis for the Thermal Dehydration in a Stream of N_2–H_2O mixed gas

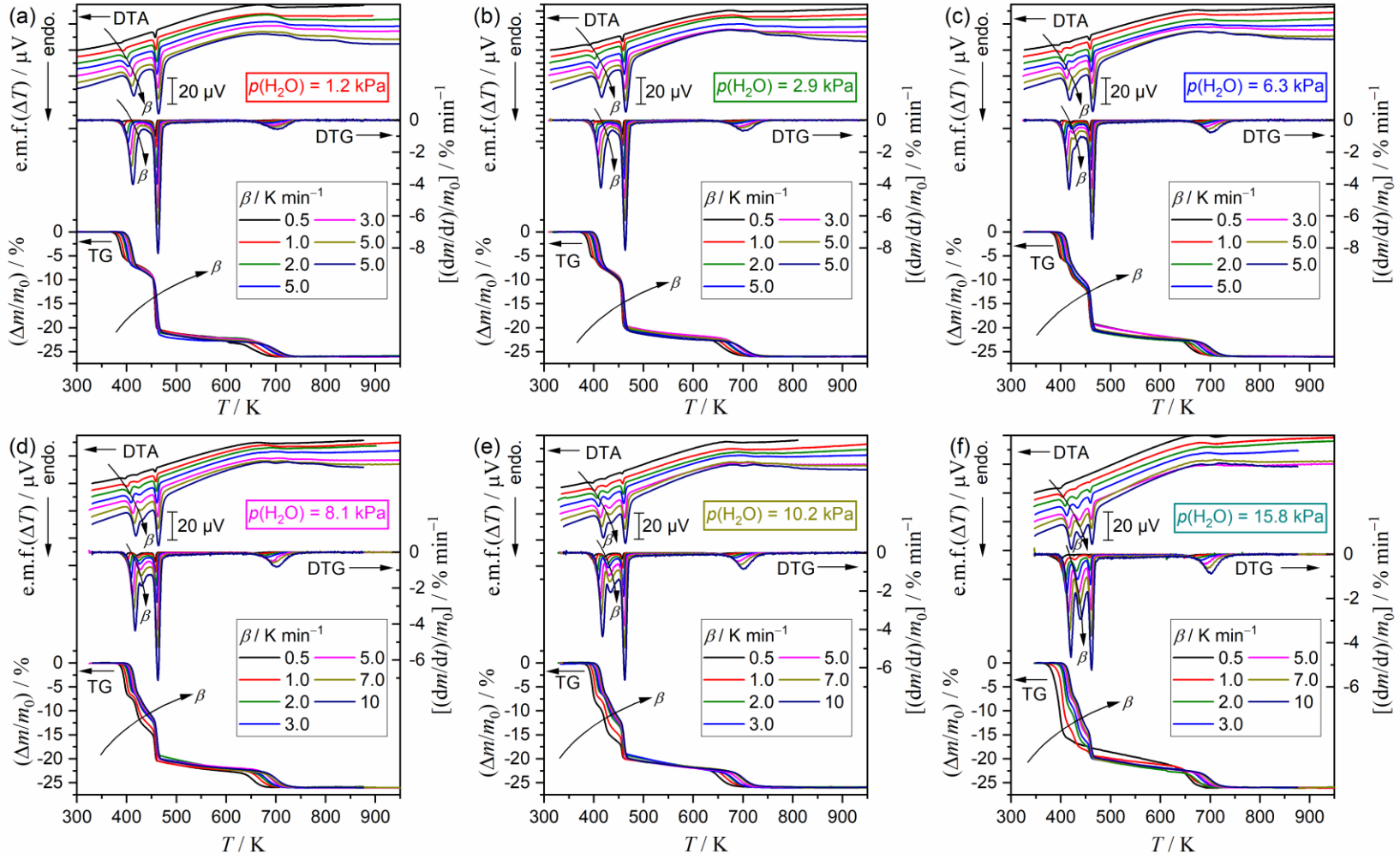

Figure S13. TG–DTG–DTA curves for the thermal dehydration of DCPD (63–75 μm; m_0 = 5.01 ± 0.03 mg) recorded at different β values in a stream of N_2–H_2O mixed gas (q_v = 200 cm^3 min^{-1}) with different $p(H_2O)$ values: (a) 1.2 kPa, (b) 2.9 kPa, (c) 6.3 kPa, (d) 8.1 kPa, (e) 10.2 kPa, and (f) 15.8 kPa.

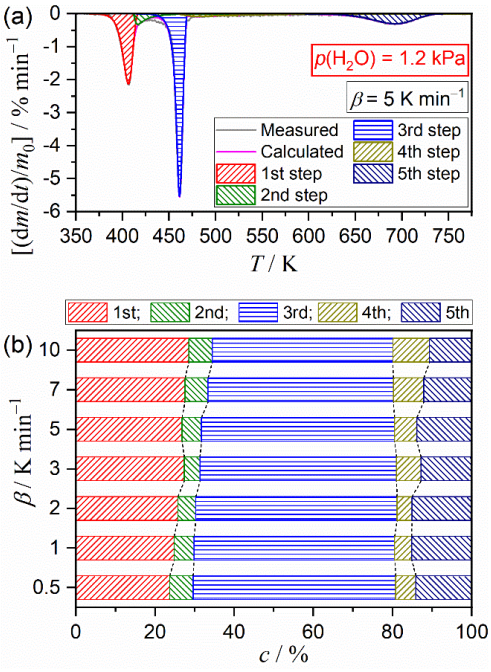

Figure S14. Result of MDA for the multistep thermal dehydration of DCPD (63–75 μm) in a stream of N_2–H_2O mixed gas with $p(H_2O)$ = 1.2 kPa: (a) typical fitting results for the overall reaction under linear nonisothermal conditions at a β of 5 K min^{-1} and (b) contributions of individual steps at various β values.

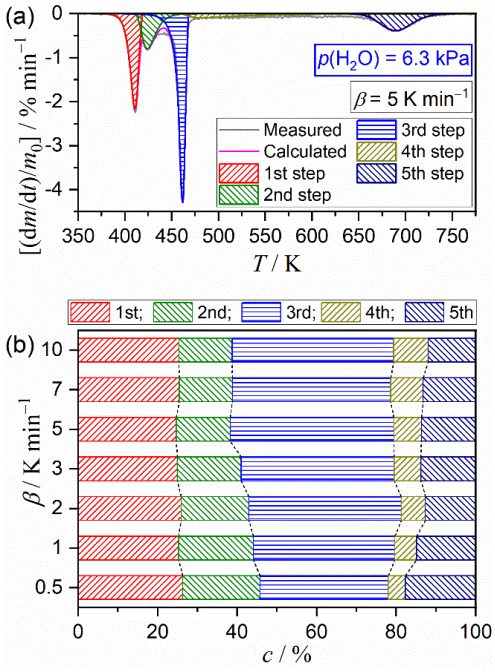

Figure S16. Result of MDA for the multistep thermal dehydration of DCPD (63–75 μm) in a stream of N_2–H_2O mixed gas with $p(H_2O)$ = 6.3 kPa: (a) typical fitting results for the overall reaction under linear nonisothermal conditions at a β of 5 K min^{-1} and (b) contributions of individual steps at various β values.

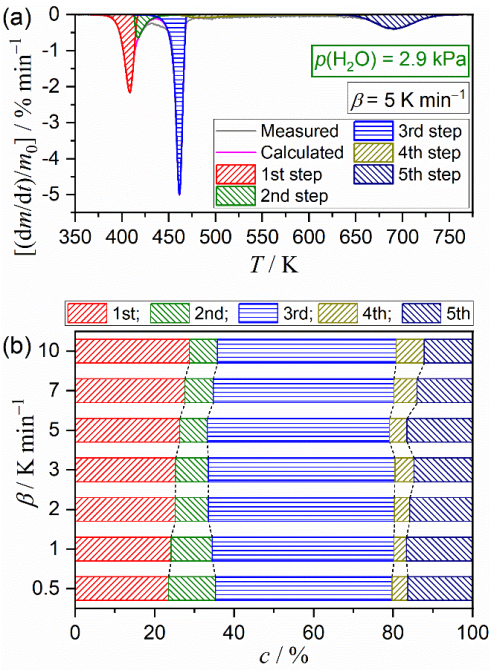

Figure S15. Result of MDA for the multistep thermal dehydration of DCPD (63–75 μm) in a stream of N_2–H_2O mixed gas with $p(H_2O)$ = 2.9 kPa: (a) typical fitting results for the overall reaction under linear nonisothermal conditions at a β of 5 K min^{-1} and (b) contributions of individual steps at various β values.

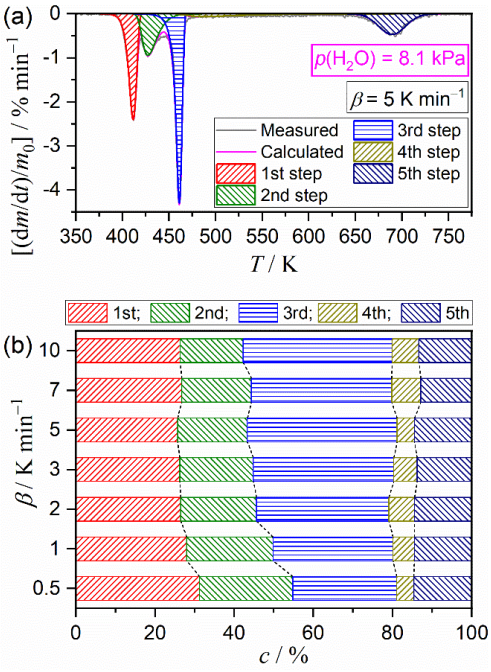

Figure S17. Result of MDA for the multistep thermal dehydration of DCPD (63–75 μm) in a stream of N_2–H_2O mixed gas with $p(H_2O)$ = 8.1 kPa: (a) typical fitting results for the overall reaction under linear nonisothermal conditions at a β of 5 K min^{-1} and (b) contributions of individual steps at various β values.

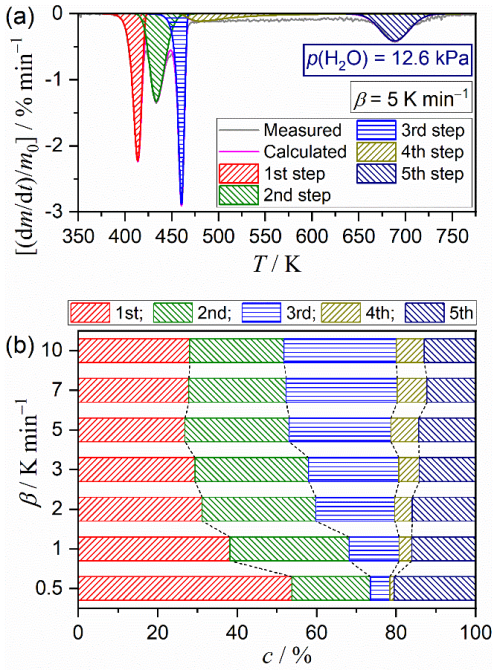

Figure S19. Result of MDA for the multistep thermal dehydration of DCPD (63–75 μm) in a stream of N_2–H_2O mixed gas with $p(H_2O)$ = 12.6 kPa: (a) typical fitting results for the overall reaction under linear nonisothermal conditions at a β of 5 K min^{-1} and (b) contributions of individual steps at various β values.

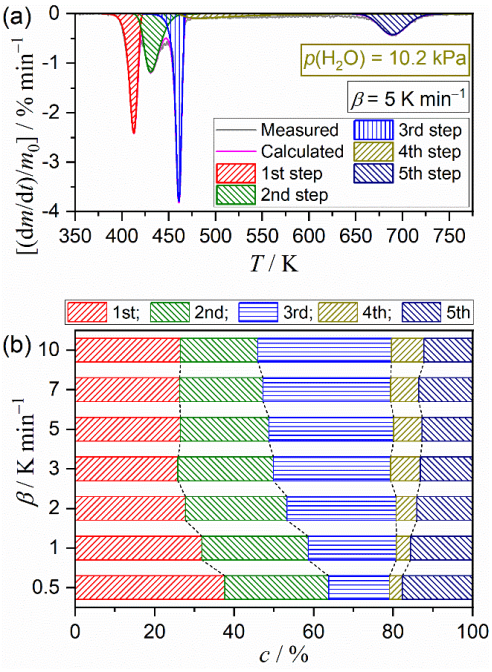

Figure S18. Result of MDA for the multistep thermal dehydration of DCPD (63–75 μm) in a stream of N_2–H_2O mixed gas with $p(H_2O)$ = 10.2 kPa: (a) typical fitting results for the overall reaction under linear nonisothermal conditions at a β of 5 K min^{-1} and (b) contributions of individual steps at various β values.

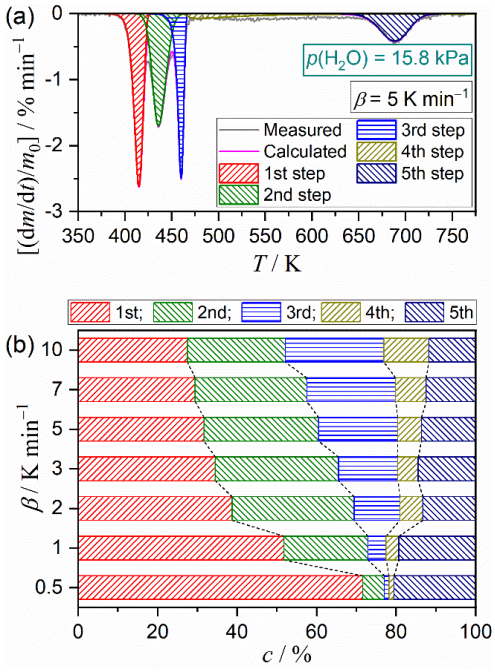

Figure S20. Result of MDA for the multistep thermal dehydration of DCPD (63–75 μm) in a stream of N_2–H_2O mixed gas with $p(H_2O)$ = 15.8 kPa: (a) typical fitting results for the overall reaction under linear nonisothermal conditions at a β of 5 K min^{-1} and (b) contributions of individual steps at various β values.

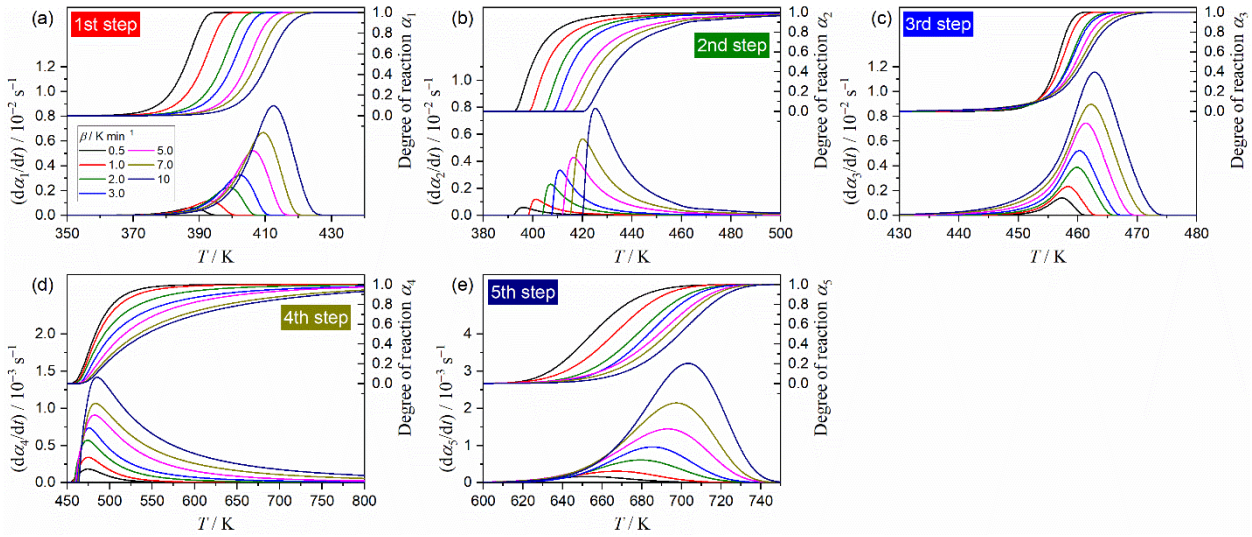

Figure S21. Kinetic curves for each reaction step of the multistep thermal dehydration of DCPD (63–75 μm) in a stream of N_2–H_2O mixed gas with $p(H_2O)$ = 1.2 kPa: (a) first, (b) second, (c) third, (d) fourth, and (e) fifth steps.

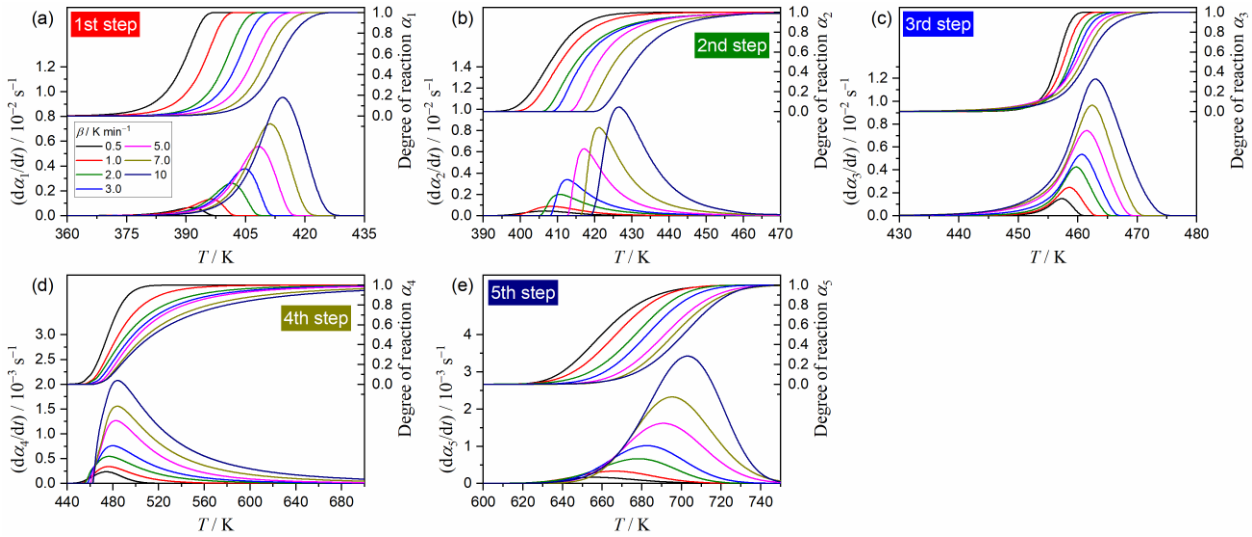

Figure S22. Kinetic curves for each reaction step of the multistep thermal dehydration of DCPD (63–75 μm) in a stream of N_2–H_2O mixed gas with $p(H_2O)$ = 2.9 kPa: (a) first, (b) second, (c) third, (d) fourth, and (e) fifth steps.

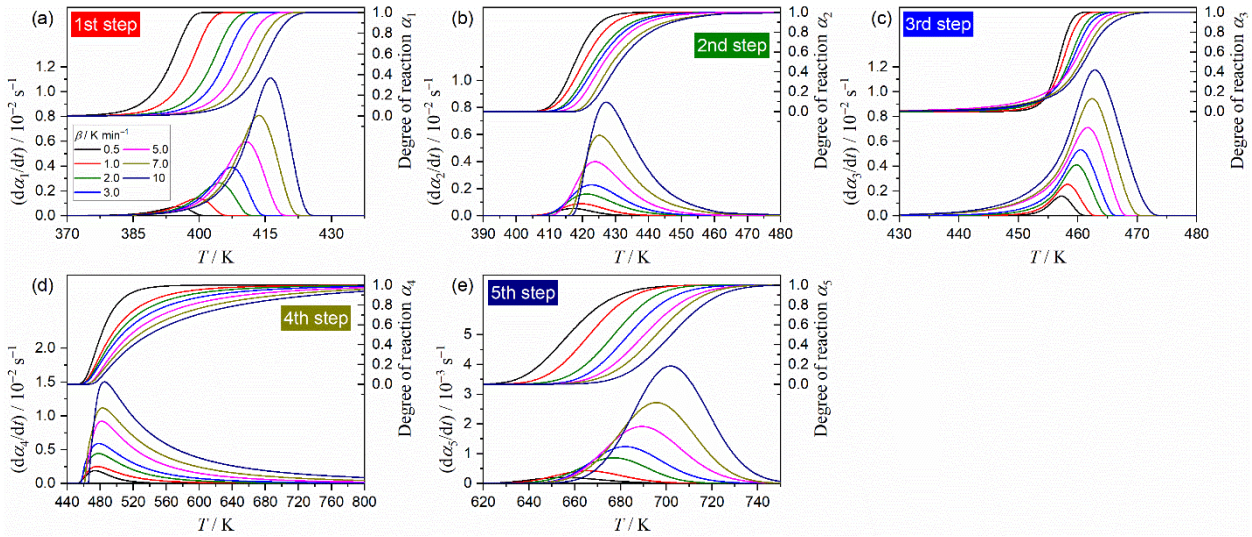

Figure S23. Kinetic curves for each reaction step of the multistep thermal dehydration of DCPD (63–75 μm) in a stream of N_2–H_2O mixed gas with $p(H_2O)$ = 6.3 kPa: (a) first, (b) second, (c) third, (d) fourth, and (e) fifth steps.

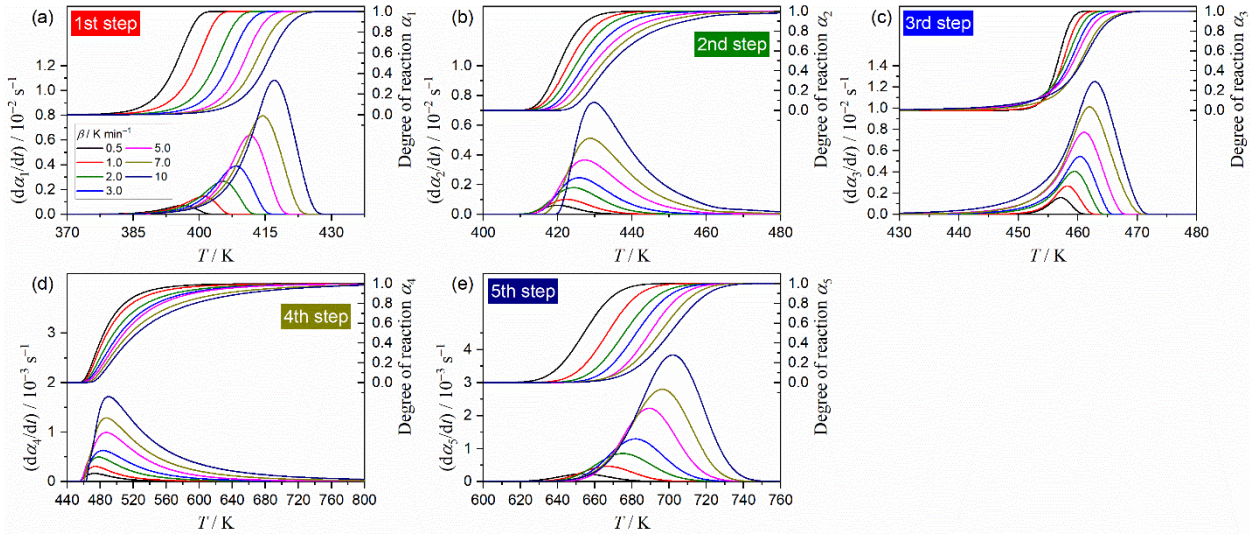

Figure S24. Kinetic curves for each reaction step of the multistep thermal dehydration of DCPD (63–75 μm) in a stream of N_2–H_2O mixed gas with $p(H_2O)$ = 8.1 kPa: (a) first, (b) second, (c) third, (d) fourth, and (e) fifth steps.

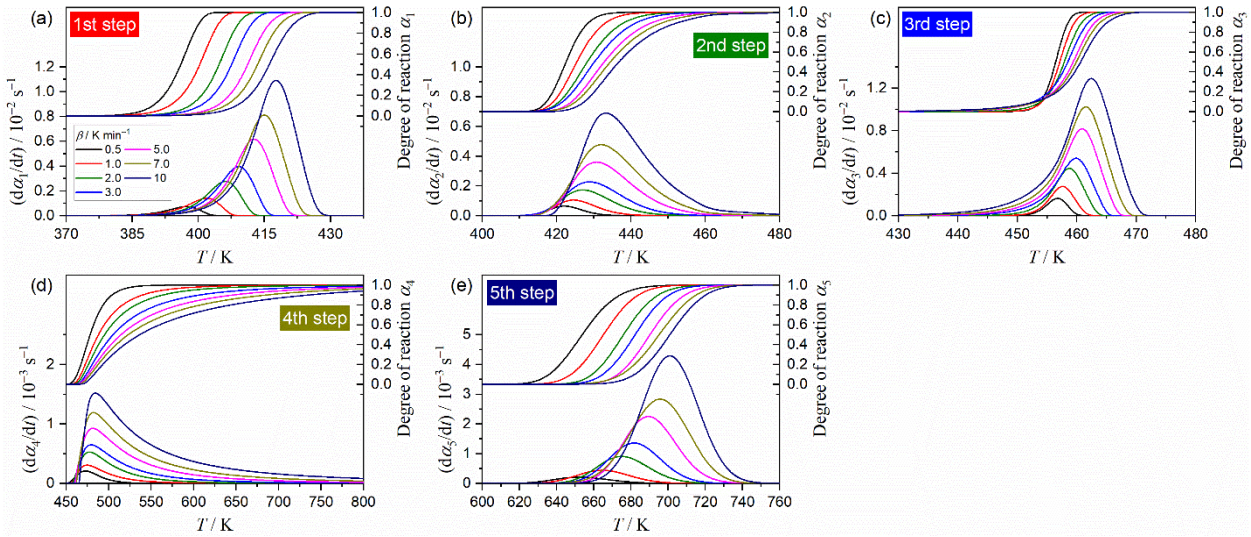

Figure S25. Kinetic curves for each reaction step of the multistep thermal dehydration of DCPD (63–75 μm) in a stream of N_2–H_2O mixed gas with $p(H_2O)$ = 10.2 kPa: (a) first, (b) second, (c) third, (d) fourth, and (e) fifth steps.

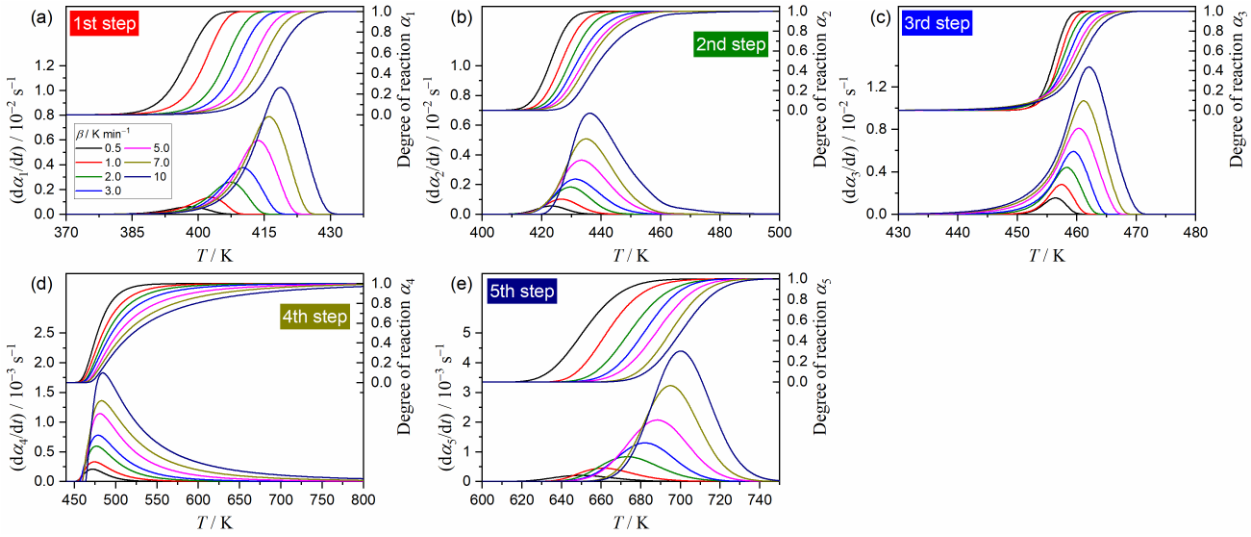

Figure S26. Kinetic curves for each reaction step of the multistep thermal dehydration of DCPD (63–75 μm) in a stream of N_2–H_2O mixed gas with $p(H_2O)$ = 12.6 kPa: (a) first, (b) second, (c) third, (d) fourth, and (e) fifth steps.

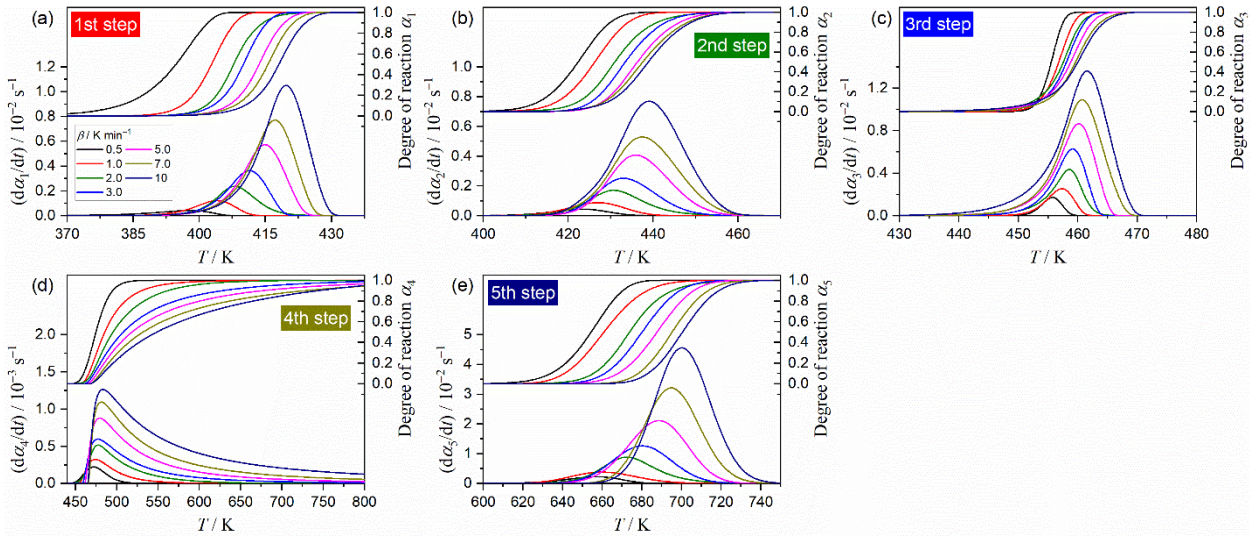

Figure S27. Kinetic curves for each reaction step of the multistep thermal dehydration of DCPD (63–75 μm) in a stream of N_2–H_2O mixed gas with $p(H_2O)$ = 15.8 kPa: (a) first, (b) second, (c) third, (d) fourth, and (e) fifth steps.

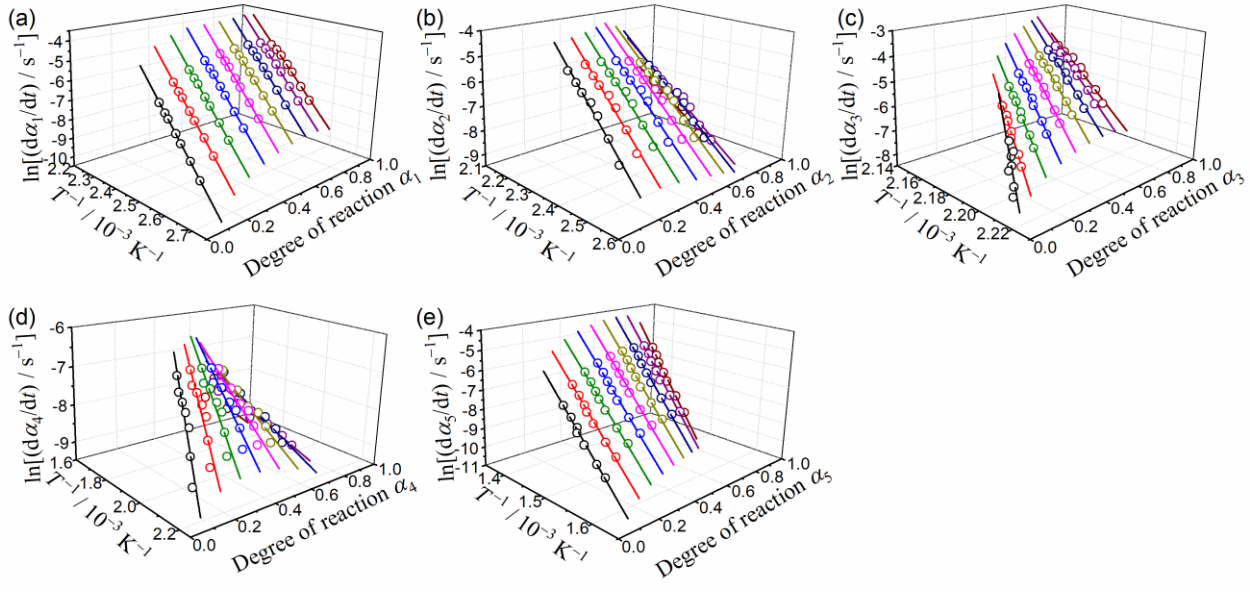

Figure S28. Friedman plots for each step of the multistep thermal dehydration of DCPD (63–75 μm) in a stream of N_2–H_2O mixed gas with $p(H_2O)$ = 1.2 kPa: (a) first, (b) second, (c) third, (d) fourth, and (e) fifth steps.

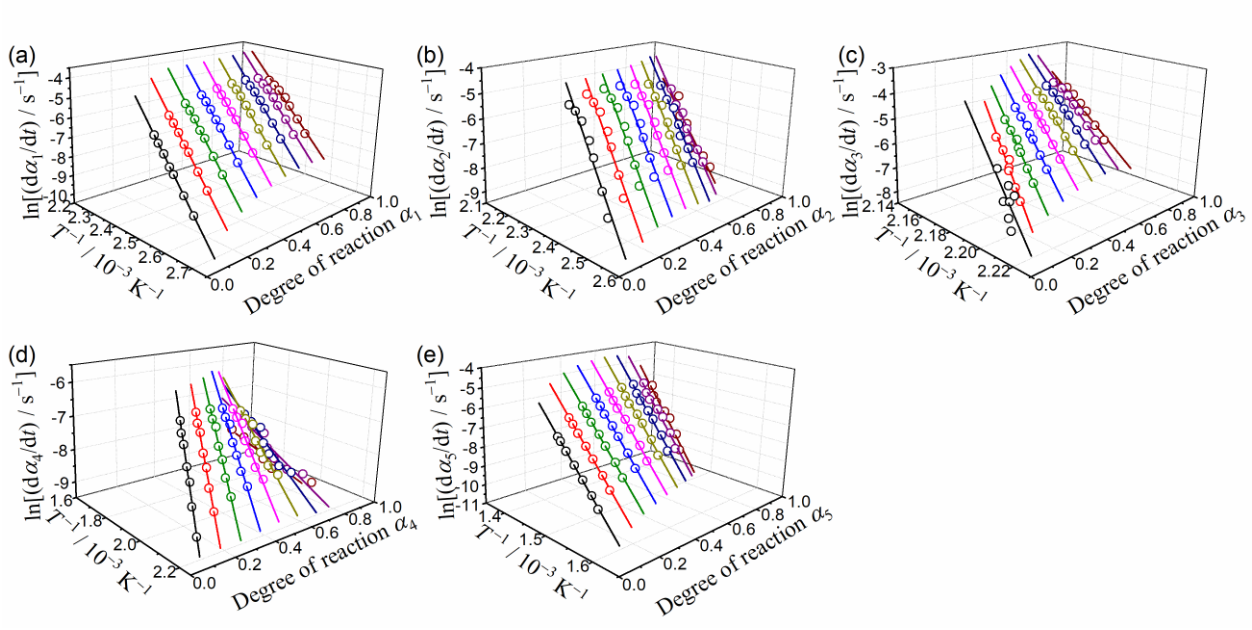

Figure S29. Friedman plots for each step of the multistep thermal dehydration of DCPD (63–75 μm) in a stream of N_2–H_2O mixed gas with $p(H_2O)$ = 2.9 kPa: (a) first, (b) second, (c) third, (d) fourth, and (e) fifth steps.

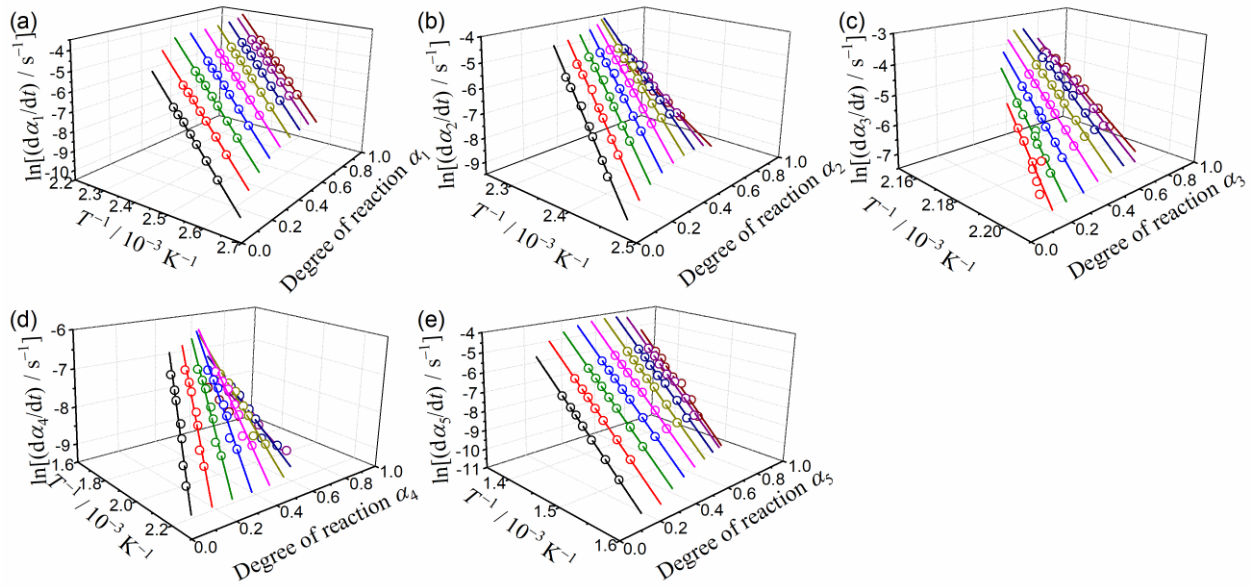

Figure S30. Friedman plots for each step of the multistep thermal dehydration of DCPD (63–75 μm) in a stream of N_2–H_2O mixed gas with $p(H_2O)$ = 6.3 kPa: (a) first, (b) second, (c) third, (d) fourth, and (e) fifth steps.

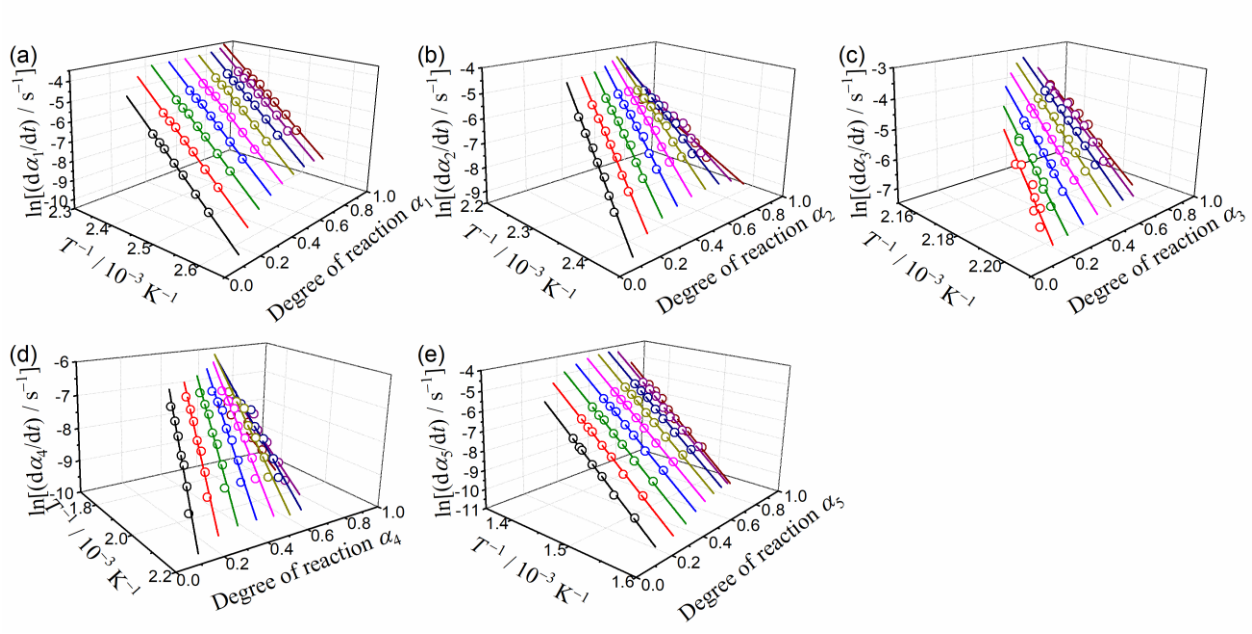

Figure S31. Friedman plots for each step of the multistep thermal dehydration of DCPD (63–75 μm) in a stream of N_2–H_2O mixed gas with $p(H_2O)$ = 8.1 kPa: (a) first, (b) second, (c) third, (d) fourth, and (e) fifth steps.

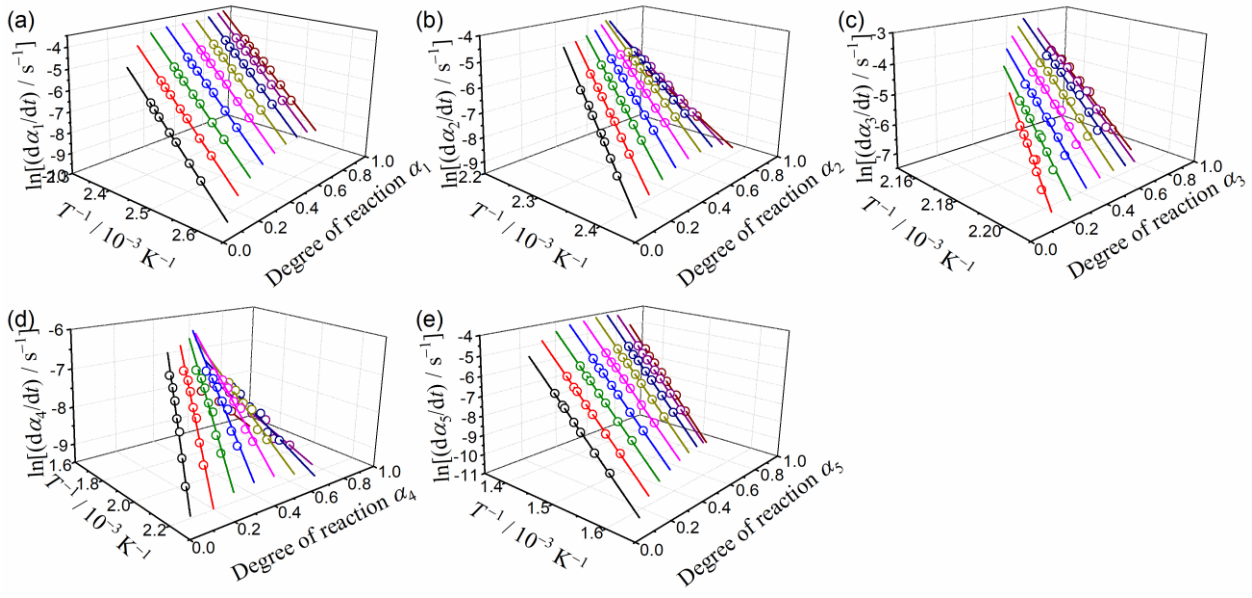

Figure S32. Friedman plots for each step of the multistep thermal dehydration of DCPD (63–75 μm) in a stream of N_2–H_2O mixed gas with $p(H_2O)$ = 10.2 kPa: (a) first, (b) second, (c) third, (d) fourth, and (e) fifth steps.

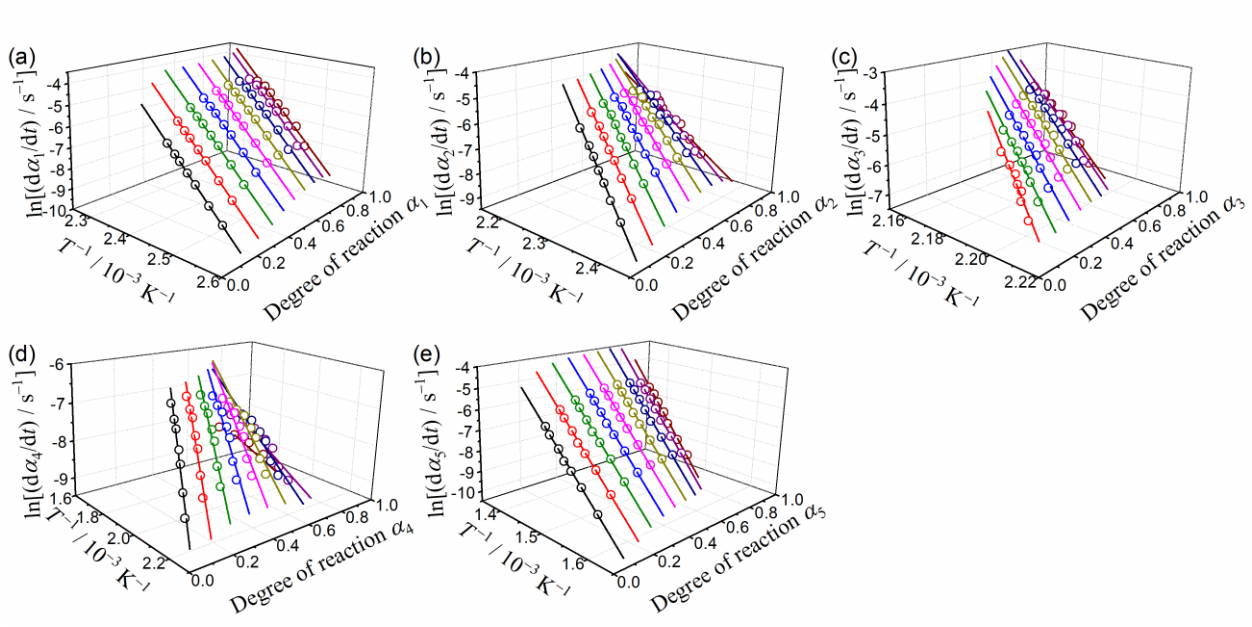

Figure S33. Friedman plots for each step of the multistep thermal dehydration of DCPD (63–75 μm) in a stream of N_2–H_2O mixed gas with $p(H_2O)$ = 12.6 kPa: (a) first, (b) second, (c) third, (d) fourth, and (e) fifth steps.

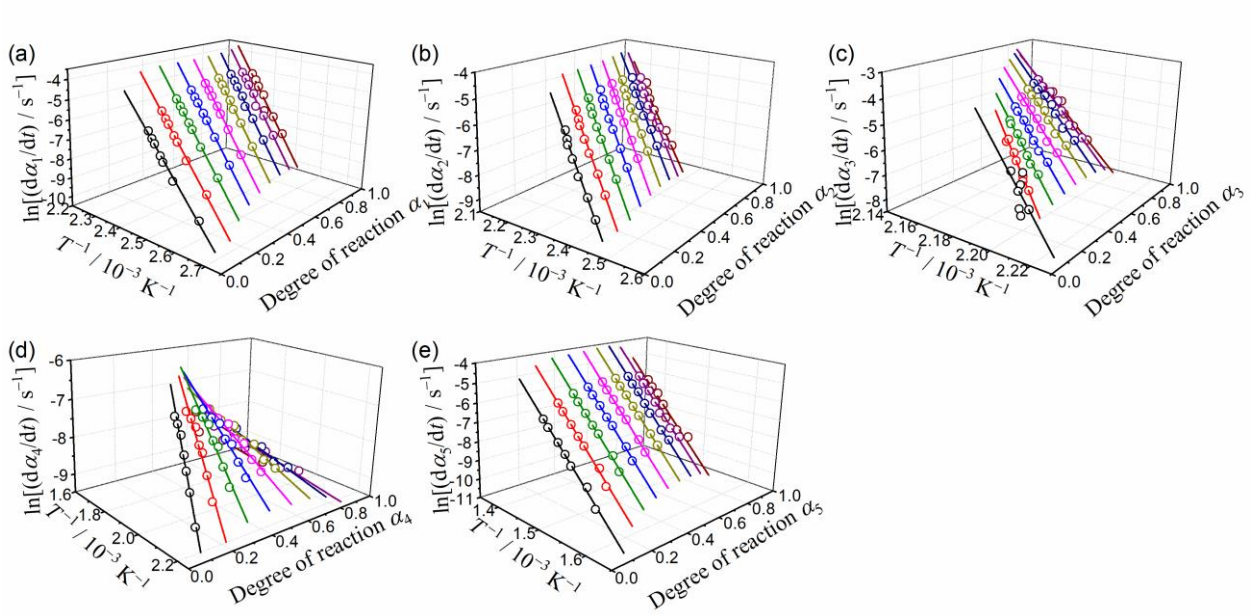

Figure S34. Friedman plots for each step of the multistep thermal dehydration of DCPD (63–75 μm) in a stream of N_2–H_2O mixed gas with $p(H_2O)$ = 15.8 kPa: (a) first, (b) second, (c) third, (d) fourth, and (e) fifth steps.

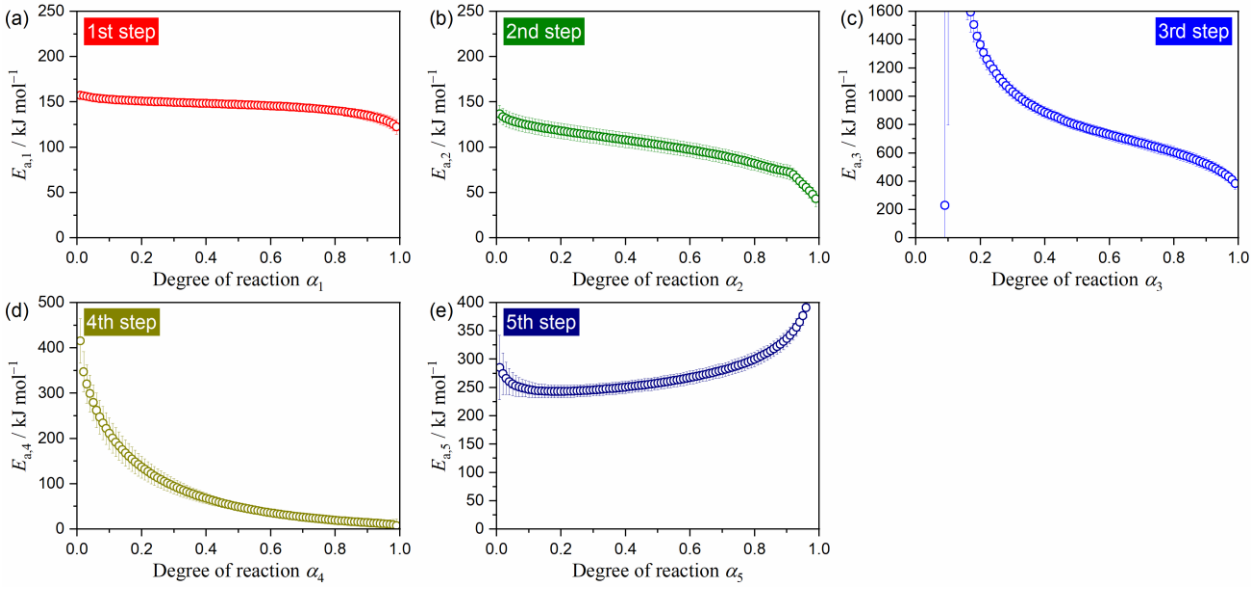

Figure S35. $E_{a,i}$ values at various α_i for each step of the multistep thermal dehydration of DCPD (63–75 μm) in a stream of N_2–H_2O mixed gas with $p(H_2O)$ = 1.2 kPa: (a) first, (b) second, (c) third, (d) fourth, and (e) fifth steps.

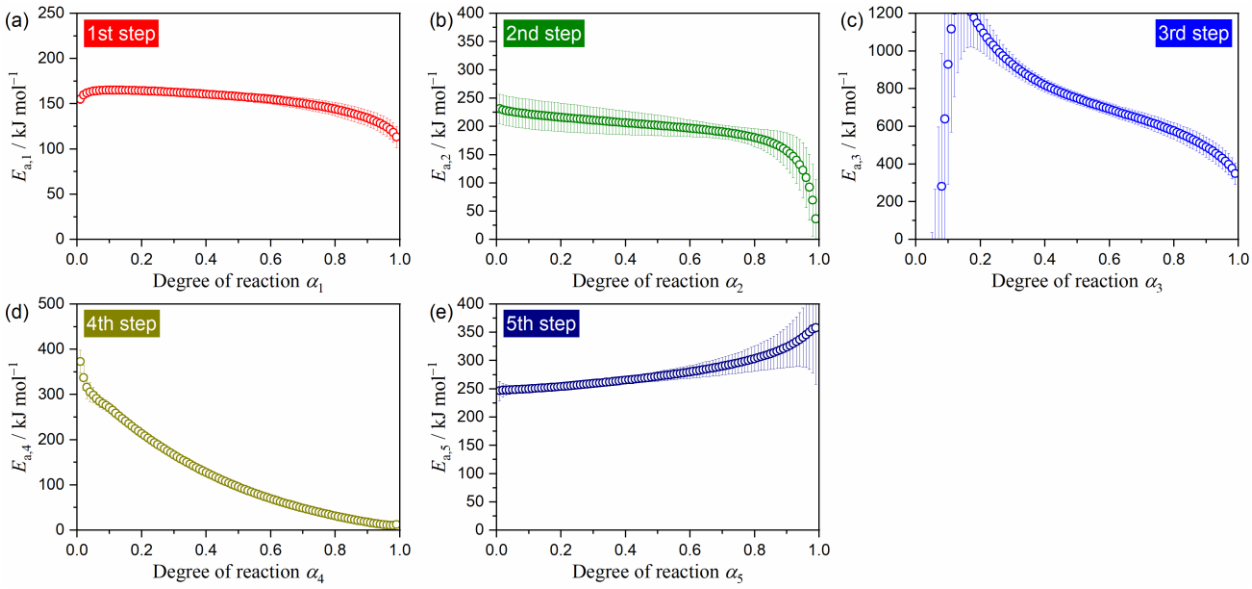

Figure S36. $E_{a,i}$ values at various α_i for each step of the multistep thermal dehydration of DCPD (63–75 μm) in a stream of N_2–H_2O mixed gas with $p(H_2O)$ = 2.9 kPa: (a) first, (b) second, (c) third, (d) fourth, and (e) fifth steps.

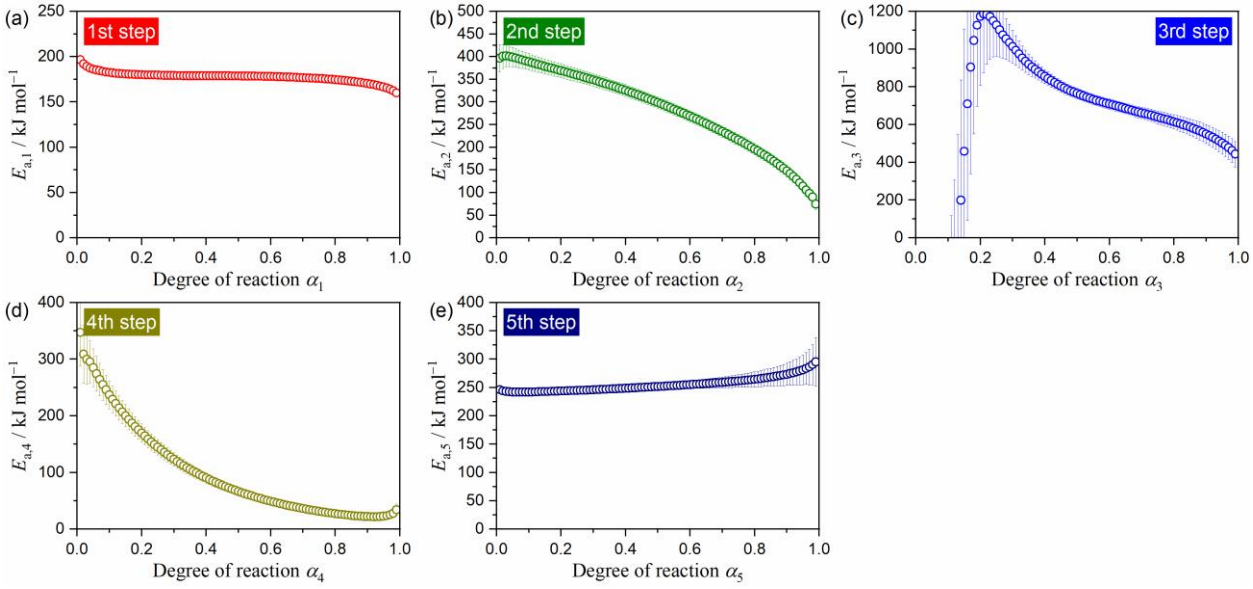

Figure S37. $E_{a,i}$ values at various α_i for each step of the multistep thermal dehydration of DCPD (63–75 μm) in a stream of N_2–H_2O mixed gas with $p(H_2O)$ = 6.3 kPa: (a) first, (b) second, (c) third, (d) fourth, and (e) fifth steps.

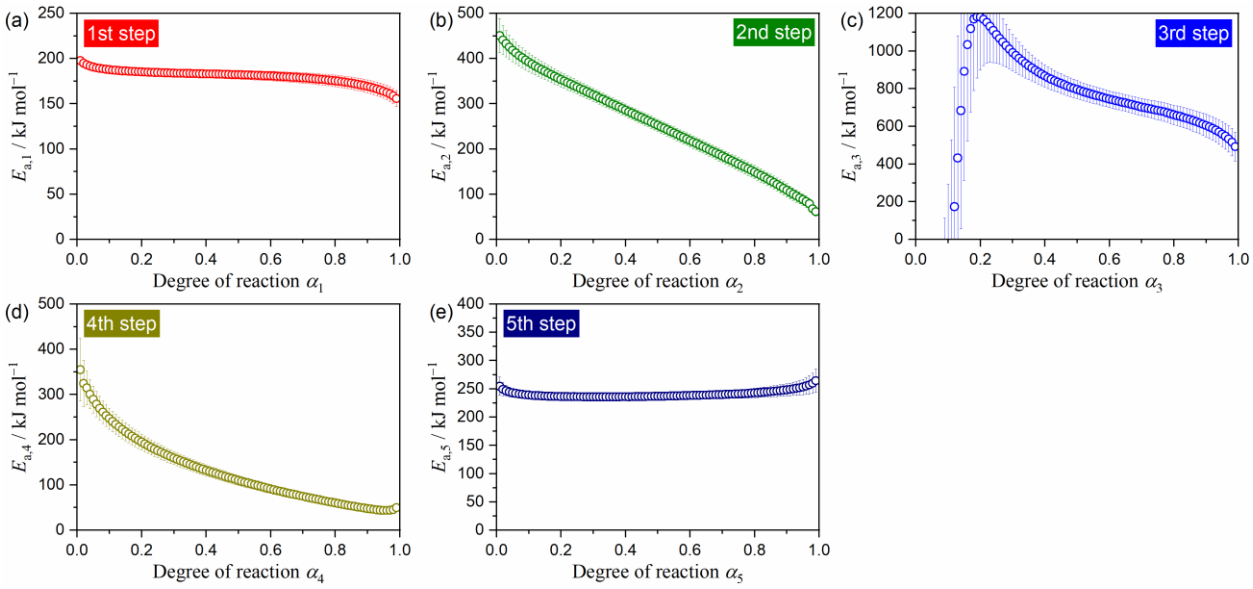

Figure S38. $E_{a,i}$ values at various α_i for each step of the multistep thermal dehydration of DCPD (63–75 μm) in a stream of N_2–H_2O mixed gas with $p(H_2O)$ = 8.1 kPa: (a) first, (b) second, (c) third, (d) fourth, and (e) fifth steps.

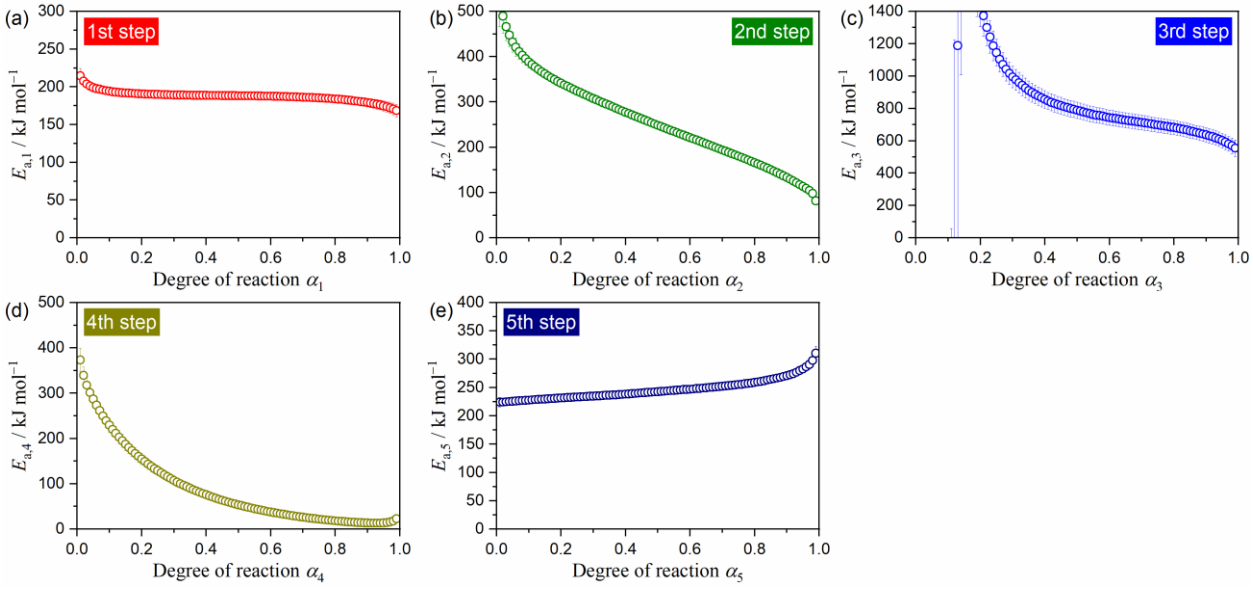

Figure S39. $E_{a,i}$ values at various α_i for each step of the multistep thermal dehydration of DCPD (63–75 μm) in a stream of N_2–H_2O mixed gas with $p(H_2O)$ = 10.2 kPa: (a) first, (b) second, (c) third, (d) fourth, and (e) fifth steps.

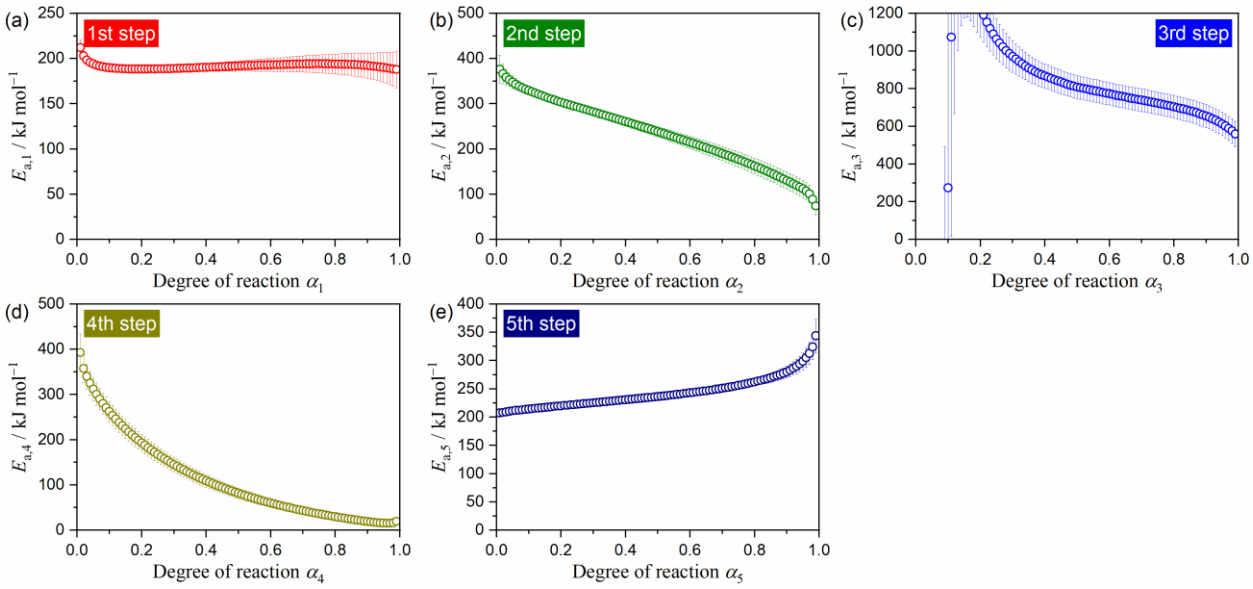

Figure S40. $E_{a,i}$ values at various α_i for each step of the multistep thermal dehydration of DCPD (63–75 μm) in a stream of N_2–H_2O mixed gas with $p(H_2O)$ = 12.6 kPa: (a) first, (b) second, (c) third, (d) fourth, and (e) fifth steps.

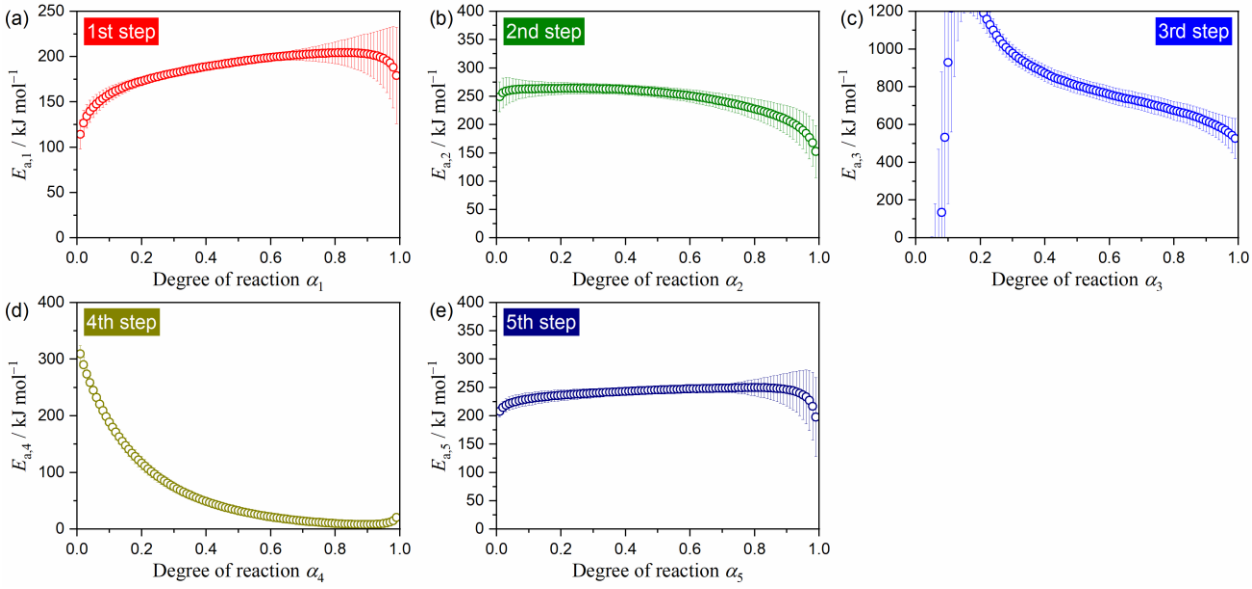

Figure S41. $E_{a,i}$ values at various α_i for each step of the multistep thermal dehydration of DCPD (63–75 μm) in a stream of N_2–H_2O mixed gas with $p(H_2O)$ = 15.8 kPa: (a) first, (b) second, (c) third, (d) fourth, and (e) fifth steps.

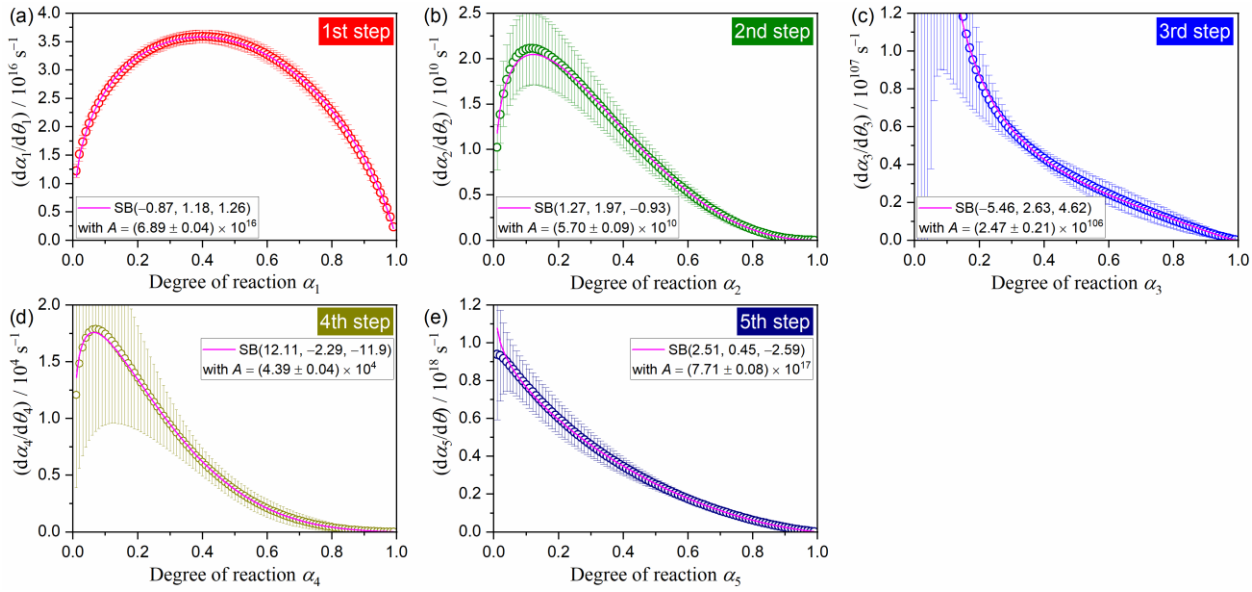

Figure S42. Experimental master plots for each step of the multistep thermal dehydration of DCPD (63–75 μm) in a stream of N_2–H_2O mixed gas with $p(H_2O)$ = 1.2 kPa: (a) first, (b) second, (c) third, (d) fourth, and (e) fifth steps.

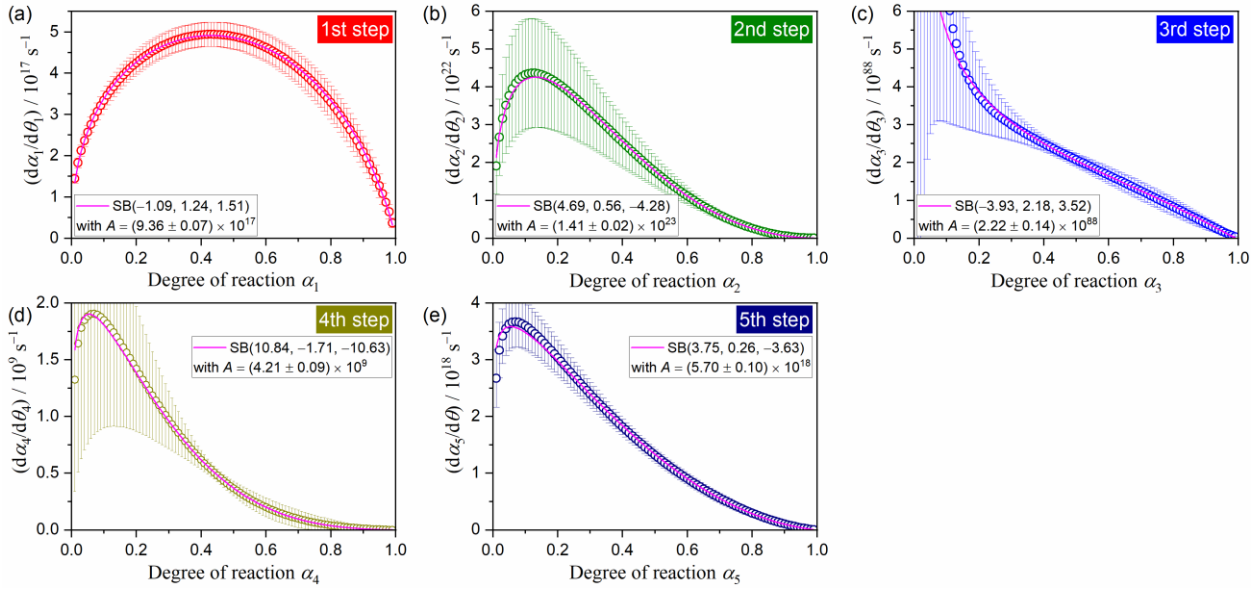

Figure S43. Experimental master plots for each step of the multistep thermal dehydration of DCPD (63–75 μm) in a stream of N_2–H_2O mixed gas with $p(H_2O)$ = 2.9 kPa: (a) first, (b) second, (c) third, (d) fourth, and (e) fifth steps.

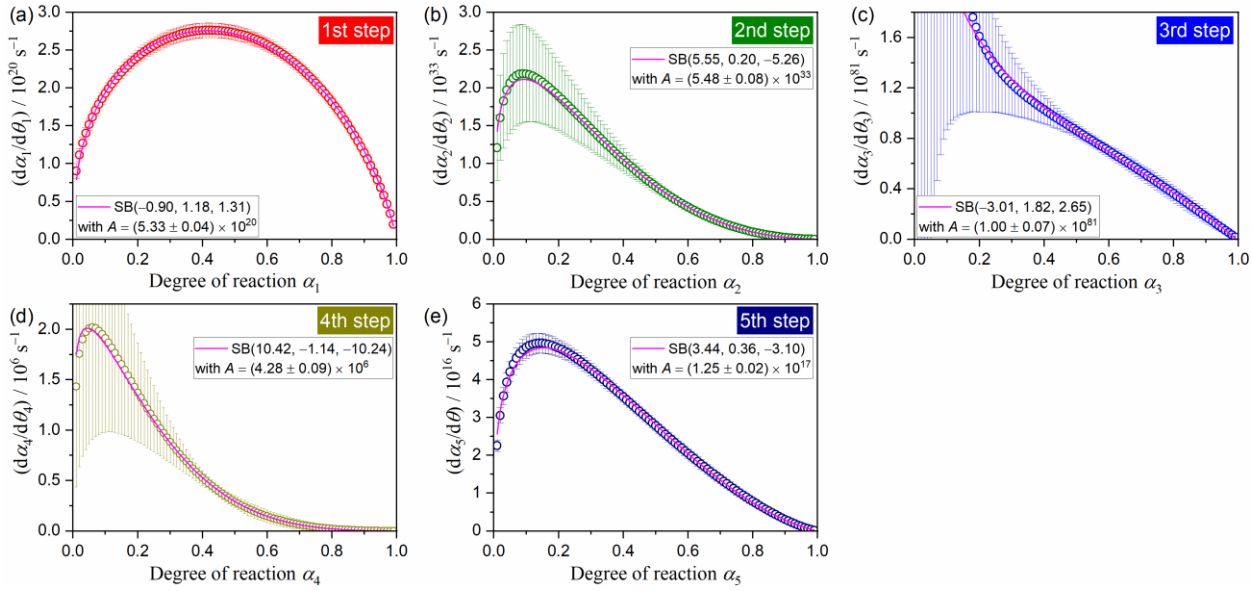

Figure S44. Experimental master plots for each step of the multistep thermal dehydration of DCPD (63–75 μm) in a stream of N_2–H_2O mixed gas with $p(H_2O)$ = 6.3 kPa: (a) first, (b) second, (c) third, (d) fourth, and (e) fifth steps.

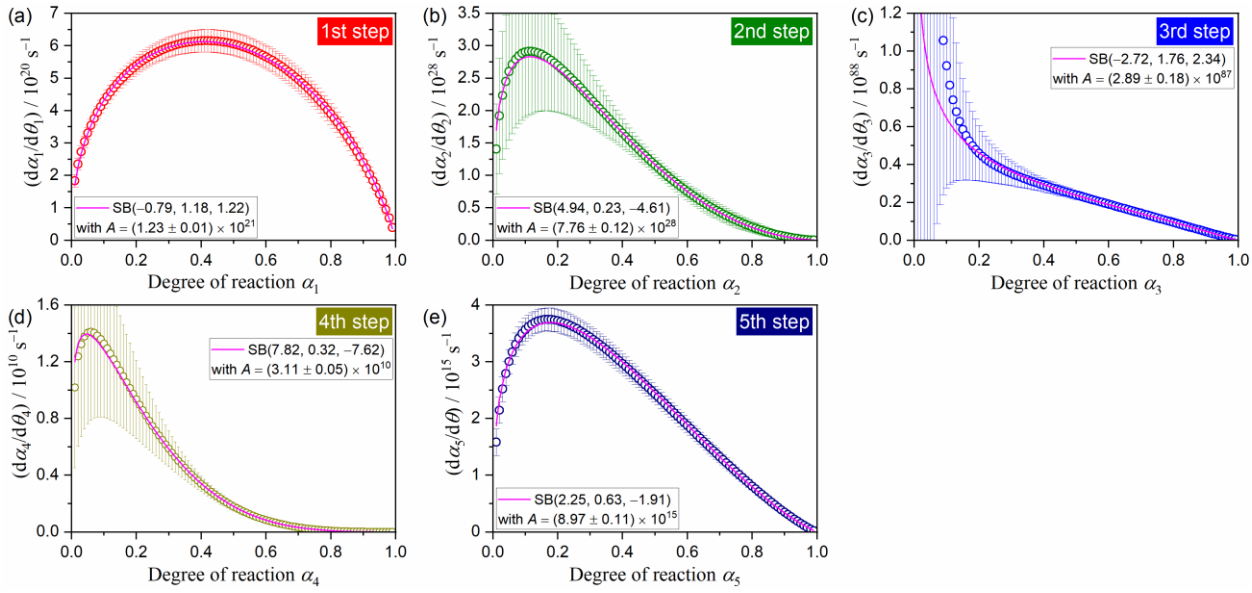

Figure S45. Experimental master plots for each step of the multistep thermal dehydration of DCPD (63–75 μm) in a stream of N_2–H_2O mixed gas with $p(H_2O)$ = 8.1 kPa: (a) first, (b) second, (c) third, (d) fourth, and (e) fifth steps.

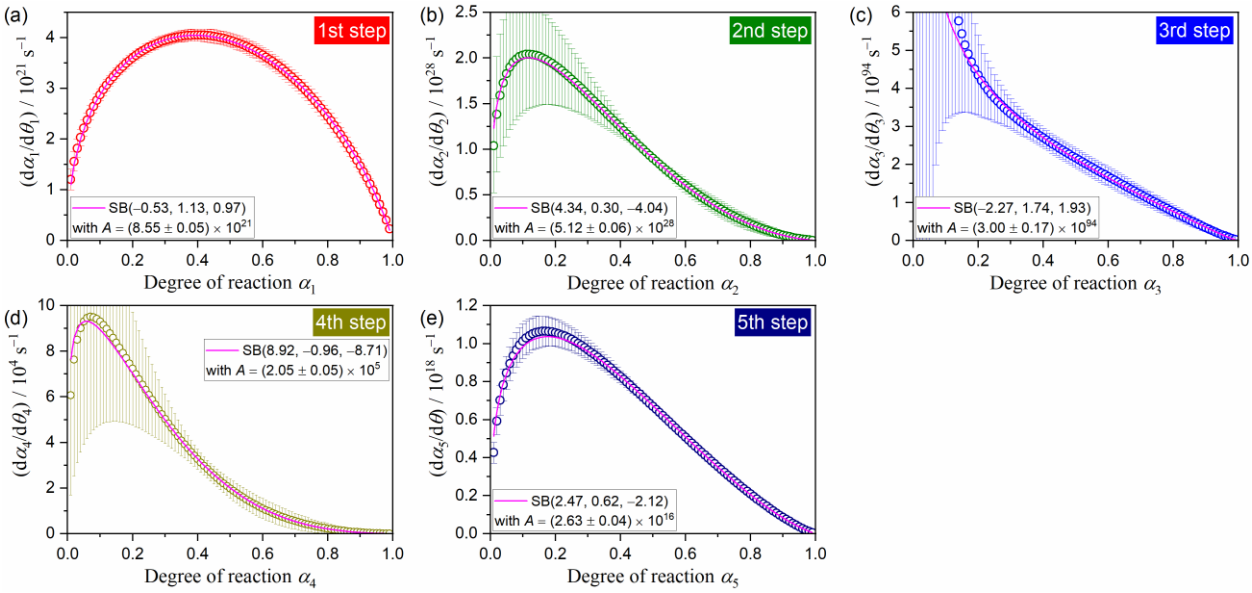

Figure S46. Experimental master plots for each step of the multistep thermal dehydration of DCPD (63–75 μm) in a stream of N_2–H_2O mixed gas with $p(H_2O)$ = 10.2 kPa: (a) first, (b) second, (c) third, (d) fourth, and (e) fifth steps.

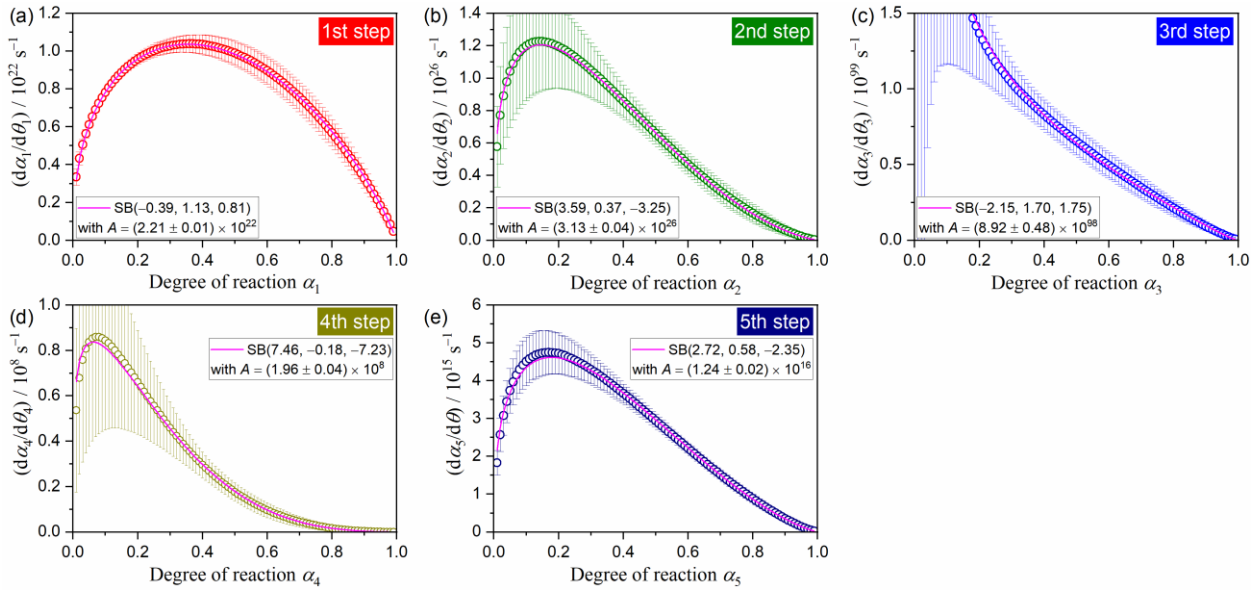

Figure S47. Experimental master plots for each step of the multistep thermal dehydration of DCPD (63–75 μm) in a stream of N_2–H_2O mixed gas with $p(H_2O)$ = 12.6 kPa: (a) first, (b) second, (c) third, (d) fourth, and (e) fifth steps.

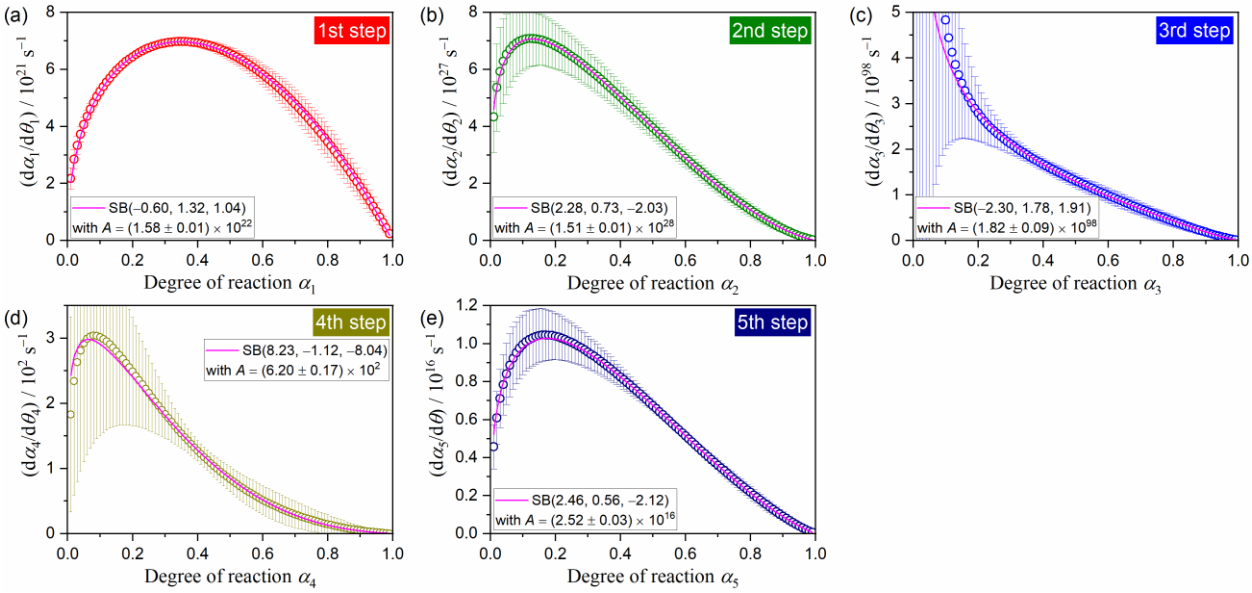

Figure S48. Experimental master plots for each step of the multistep thermal dehydration of DCPD (63–75 μm) in a stream of N_2–H_2O mixed gas with $p(H_2O)$ = 15.8 kPa: (a) first, (b) second, (c) third, (d) fourth, and (e) fifth steps.

Table S5. Results of mathematical deconvolution analysis and subsequent formal kinetic analysis for the multistep thermal dehydration of DCPD (63–75 μm) in a stream of N_2–H_2O mixed gas with $p(H_2O)$ = 1.2 kPa

i	$E_{a,i}$/ kJ mol^{-1}, [a]	$\frac{d\alpha_i}{d\theta_i} = A_i f(\alpha_i)$ with $f(\alpha_i) = \alpha_i^{m_i}(1-\alpha_i)^{n_i}[-\ln(1-\alpha_i)]^{p_i}$				
		A_i / s^{-1}	m_i	n_i	p_i	R^{2}, [b]
1	146.2 ± 4.5	(6.89 ± 0.04) × 10^{16}	−0.87 ± 0.07	1.18 ± 0.03	1.26 ± 0.06	0.9997
2	101.2 ± 14.3	(5.70 ± 0.09) × 10^{10}	1.27 ± 0.16	1.97 ± 0.06	–0.93 ± 0.16	0.9996
3	956.6 ± 477.5	(2.47 ± 0.21) × 10^{106}	−5.46 ± 0.79	2.63 ± 0.29	4.62 ± 0.75	0.9981
4	67.3 ± 51.8	(4.39± 0.04) × 10^{4}	12.11 ± 0.15	–2.29 ± 0.06	–11.87 ± 0.14	0.9999
5	266.6 ± 25.0	(7.71 ± 0.08) × 10^{17}	2.51 ± 0.10	0.45 ± 0.04	–2.59 ± 0.10	0.9998

[a]Average value over $0.1 \le \alpha \le 0.9$.
[b]Determination coefficient of the nonlinear least-squares analysis for fitting the experimental master plot.

Table S6. Results of mathematical deconvolution analysis and subsequent formal kinetic analysis for the multistep thermal dehydration of DCPD (63–75 μm) in a stream of N_2–H_2O mixed gas with $p(H_2O)$ = 2.9 kPa

i	$E_{a,i}$/ kJ mol^{-1}, [a]	$\frac{d\alpha_i}{d\theta_i} = A_i f(\alpha_i)$ with $f(\alpha_i) = \alpha_i^{m_i}(1-\alpha_i)^{n_i}[-\ln(1-\alpha_i)]^{p_i}$				
		A_i / s^{-1}	m_i	n_i	p_i	R^{2}, [b]
1	155.6 ± 8.6	(9.36 ± 0.07) × 10^{17}	−1.09 ± 0.09	1.24 ± 0.04	1.51 ± 0.08	0.9993
2	199.1 ± 15.5	(1.41 ± 0.02) × 10^{23}	4.69 ± 0.14	0.56 ± 0.06	–4.28 ± 0.14	0.9998
3	797.0 ± 210.5	(2.22 ± 0.14) × 10^{88}	−3.93 ± 0.54	2.18 ± 0.19	3.52 ± 0.51	0.9985
4	112.1 ± 73.4	(4.21± 0.09) × 10^{9}	10.84 ± 0.29	–1.71 ± 0.12	–10.63 ± 0.28	0.9996
5	276.2 ± 20.2	(5.70 ± 0.10) × 10^{18}	3.75 ± 0.19	0.26 ± 0.07	–3.63 ± 0.18	0.9995

[a]Average value over $0.1 \le \alpha \le 0.9$.
[b]Determination coefficient of the nonlinear least-squares analysis for fitting the experimental master plot.

Table S7. Results of mathematical deconvolution analysis and subsequent formal kinetic analysis for the multistep thermal dehydration of DCPD (63–75 μm) in a stream of N_2–H_2O mixed gas with $p(H_2O)$ = 6.3 kPa

i	$E_{a,i}$/ kJ mol^{-1}, [a]	$\frac{d\alpha_i}{d\theta_i} = A_i f(\alpha_i)$ with $f(\alpha_i) = \alpha_i^{m_i}(1-\alpha_i)^{n_i}[-\ln(1-\alpha_i)]^{p_i}$				
		A_i / s^{-1}	m_i	n_i	p_i	R^{2}, [b]
1	177.8 ± 2.6	(5.33 ± 0.04) × 10^{20}	−0.90 ± 0.07	1.18 ± 0.03	1.31 ± 0.06	0.9996
2	288.7 ± 69.1	(5.48 ± 0.08) × 10^{33}	5.54 ± 0.17	0.20 ± 0.07	–5.26 ± 0.16	0.9998
3	731.8 ± 293.3	(1.00 ± 0.07) × 10^{81}	−3.01 ± 0.46	1.82 ± 0.15	2.65 ± 0.42	0.9987
4	86.2 ± 60.1	(4.28± 0.09) × 10^{6}	10.41 ± 0.29	–1.14 ± 0.12	–10.22 ± 0.28	0.9995
5	253.2 ± 8.6	(1.25 ± 0.02) × 10^{17}	3.43 ± 0.19	0.36 ± 0.08	–3.09 ± 0.19	0.9995

[a]Average value over $0.1 \le \alpha \le 0.9$.
[b]Determination coefficient of the nonlinear least-squares analysis for fitting the experimental master plot.

Table S8. Results of mathematical deconvolution analysis and subsequent formal kinetic analysis for the multistep thermal dehydration of DCPD (63–75 μm) in a stream of N_2–H_2O mixed gas with $p(H_2O)$ = 8.1 kPa

i	$E_{a,i}$/ kJ mol^{-1}, [a]	$\frac{d\alpha_i}{d\theta_i} = A_i f(\alpha_i)$ with $f(\alpha_i) = \alpha_i^{m_i}(1-\alpha_i)^{n_i}[-\ln(1-\alpha_i)]^{p_i}$				
		A_i / s^{-1}	m_i	n_i	p_i	R^{2}, [b]
1	180.9 ± 4.4	(1.23 ± 0.01) × 10^{21}	−0.79 ± 0.07	1.18 ± 0.03	1.22 ± 0.06	0.9997
2	251.6 ± 81.0	(7.76 ± 0.12) × 10^{28}	4.94 ± 0.15	0.23 ± 0.06	–4.61 ± 0.15	0.9998
3	788.0 ± 233.0	(2.89 ± 0.18) × 10^{87}	−2.72 ± 0.41	1.76 ± 0.14	2.34 ± 0.38	0.9985
4	121.0 ± 54.8	(3.11± 0.05) × 10^{10}	7.82 ± 0.15	0.32 ± 0.06	–7.62 ± 0.15	0.9997
5	238.6 ± 3.2	(8.97 ± 0.11) × 10^{15}	2.25 ± 0.11	0.63 ± 0.04	–1.91 ± 0.11	0.9997

[a]Average value over $0.1 \leq \alpha \leq 0.9$.
[b]Determination coefficient of the nonlinear least-squares analysis for fitting the experimental master plot.

Table S9. Results of mathematical deconvolution analysis and subsequent formal kinetic analysis for the multistep thermal dehydration of DCPD (63–75 μm) in a stream of N_2–H_2O mixed gas with $p(H_2O)$ = 10.2 kPa

i	$E_{a,i}$/ kJ mol^{-1}, [a]	$\frac{d\alpha_i}{d\theta_i} = A_i f(\alpha_i)$ with $f(\alpha_i) = \alpha_i^{m_i}(1-\alpha_i)^{n_i}[-\ln(1-\alpha_i)]^{p_i}$				
		A_i / s^{-1}	m_i	n_i	p_i	R^{2}, [b]
1	187.6 ± 3.2	(8.55 ± 0.05) × 10^{21}	−0.53 ± 0.05	1.13 ± 0.02	0.97 ± 0.05	0.9999
2	252.0 ± 70.2	(5.12 ± 0.06) × 10^{28}	4.34 ± 0.12	0.30 ± 0.05	–4.04 ± 0.12	0.9999
3	848.4 ± 459.1	(3.00 ± 0.17) × 10^{94}	−2.27 ± 0.39	1.74 ± 0.13	1.93 ± 0.36	0.9987
4	73.9 ± 58.8	(2.05± 0.05) × 10^{5}	8.90 ± 0.27	–0.95 ± 0.11	–8.70 ± 0.27	0.9995
5	244.2 ± 11.4	(2.63 ± 0.04) × 10^{16}	2.47 ± 0.13	0.62 ± 0.05	–2.12 ± 0.12	0.9998

[a]Average value over $0.1 \leq \alpha \leq 0.9$.
[b]Determination coefficient of the nonlinear least-squares analysis for fitting the experimental master plot.

Table S10. Results of mathematical deconvolution analysis and subsequent formal kinetic analysis for the multistep thermal dehydration of DCPD (63–75 μm) in a stream of N_2–H_2O mixed gas with $p(H_2O)$ = 12.6 kPa

i	$E_{a,i}$/ kJ mol^{-1}, [a]	$\frac{d\alpha_i}{d\theta_i} = A_i f(\alpha_i)$ with $f(\alpha_i) = \alpha_i^{m_i}(1-\alpha_i)^{n_i}[-\ln(1-\alpha_i)]^{p_i}$				
		A_i / s^{-1}	m_i	n_i	p_i	R^{2}, [b]
1	191.4 ± 2.2	(2.21 ± 0.01) × 10^{22}	−0.39 ± 0.05	1.13 ± 0.02	0.81 ± 0.05	0.9999
2	235.2 ± 56.1	(3.13 ± 0.04) × 10^{26}	3.59 ± 0.10	0.37 ± 0.04	–3.25 ± 0.10	0.9999
3	887.1 ± 245.1	(8.92 ± 0.48) × 10^{98}	−2.15 ± 0.39	1.70 ± 0.13	1.75 ± 0.36	0.9984
4	100.0 ± 67.6	(1.96 ± 0.04) × 10^{8}	7.46 ± 0.23	–0.18 ± 0.09	–7.23 ± 0.23	0.9994
5	239.3 ± 17.3	(1.24 ± 0.02) × 10^{16}	2.72 ± 0.14	0.58 ± 0.05	–2.35 ± 0.13	0.9997

[a]Average value over $0.1 \leq \alpha \leq 0.9$.
[b]Determination coefficient of the nonlinear least-squares analysis for fitting the experimental master plot.

Table S11. Results of mathematical deconvolution analysis and subsequent formal kinetic analysis for the multistep thermal dehydration of DCPD (63–75 μm) in a stream of N_2–H_2O mixed gas with $p(H_2O)$ = 15.8 kPa

i	$E_{a,i}$/ kJ mol^{-1}, [a]	$\frac{d\alpha_i}{d\theta_i} = A_i f(\alpha_i)$ with $f(\alpha_i) = \alpha_i^{m_i}(1-\alpha_i)^{n_i}[-\ln(1-\alpha_i)]^{p_i}$				
		A_i / s^{-1}	m_i	n_i	p_i	R^{2}, [b]
1	190.7 ± 13.1	(1.58 ± 0.01) × 10^{22}	−0.60 ± 0.09	1.32 ± 0.04	1.04 ± 0.09	0.9998
2	250.3 ± 16.0	(1.51 ± 0.01) × 10^{28}	2.28 ± 0.04	0.73 ± 0.02	–2.03 ± 0.04	0.9999
3	880.5 ± 224.0	(1.82 ± 0.09) × 10^{98}	−2.30 ± 0.36	1.78 ± 0.13	1.91 ± 0.34	0.9993
4	51.6 ± 48.1	(6.20 ± 0.17) × 10^{2}	8.23 ± 0.32	–1.12 ± 0.12	–8.04 ± 0.31	0.9993
5	243.7 ± 5.6	(2.52 ± 0.03) × 10^{16}	2.46 ± 0.09	0.56 ± 0.04	–2.12 ± 0.09	0.9999

[a]Average value over $0.1 \leq \alpha \leq 0.9$.
[b]Determination coefficient of the nonlinear least-squares analysis for fitting the experimental master plot.

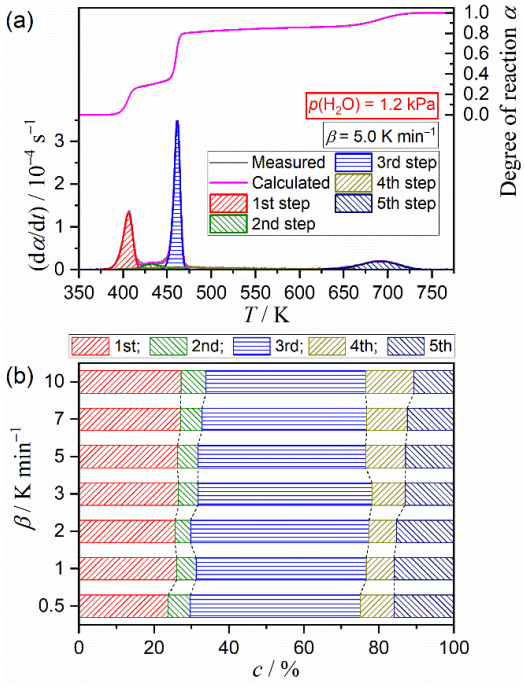

Figure S49. Results of KDA for the multistep thermal dehydration of DCPD (63–75 μm) in a stream of N_2–H_2O mixed gas with $p(H_2O)$ = 1.2 kPa: (a) typical fitting results for the overall reaction under linear nonisothermal conditions at a β of 5 K min^{-1} and (b) contributions of individual steps at various β values.

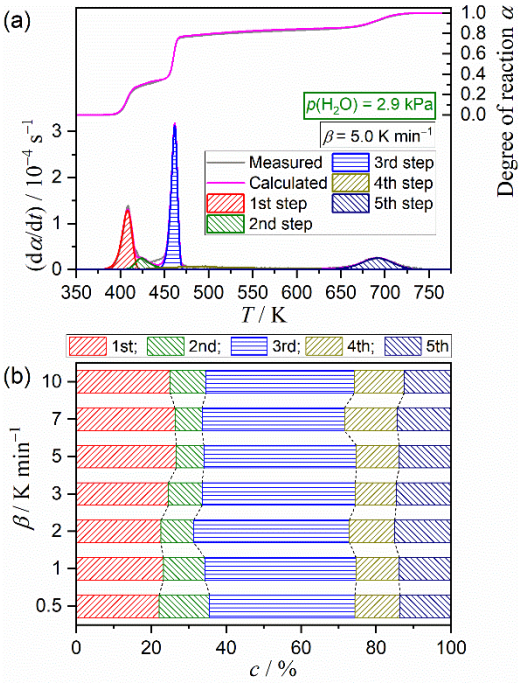

Figure S50. Results of KDA for the multistep thermal dehydration of DCPD (63–75 μm) in a stream of N_2–H_2O mixed gas with $p(H_2O)$ = 2.9 kPa: (a) typical fitting results for the overall reaction under linear nonisothermal conditions at a β of 5 K min^{-1} and (b) contributions of individual steps at various β values.

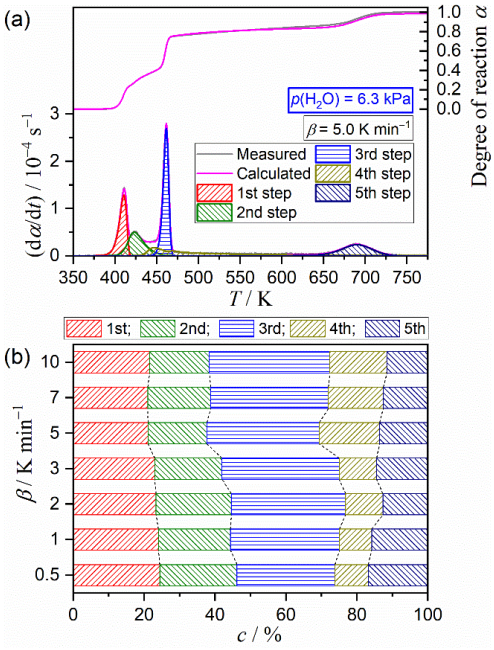

Figure S51. Results of KDA for the multistep thermal dehydration of DCPD (63–75 μm) in a stream of N_2–H_2O mixed gas with $p(H_2O)$ = 6.3 kPa: (a) typical fitting results for the overall reaction under linear nonisothermal conditions at a β of 5 K min^{-1} and (b) contributions of individual steps at various β values.

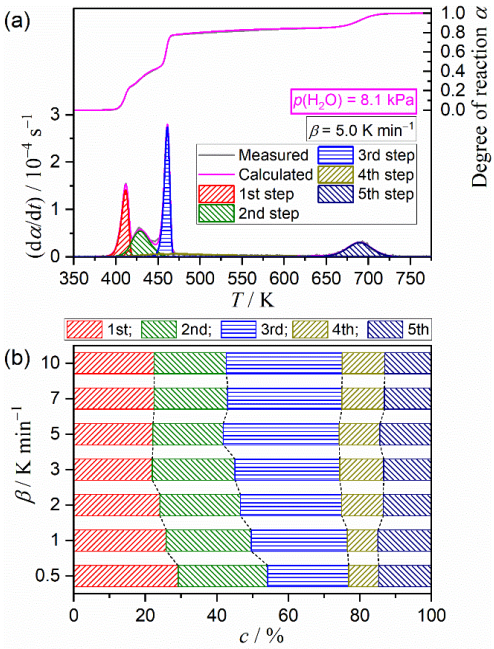

Figure S52. Results of KDA for the multistep thermal dehydration of DCPD (63–75 μm) in a stream of N_2–H_2O mixed gas with $p(H_2O)$ = 8.1 kPa: (a) typical fitting results for the overall reaction under linear nonisothermal conditions at a β of 5 K min^{-1} and (b) contributions of individual steps at various β values.

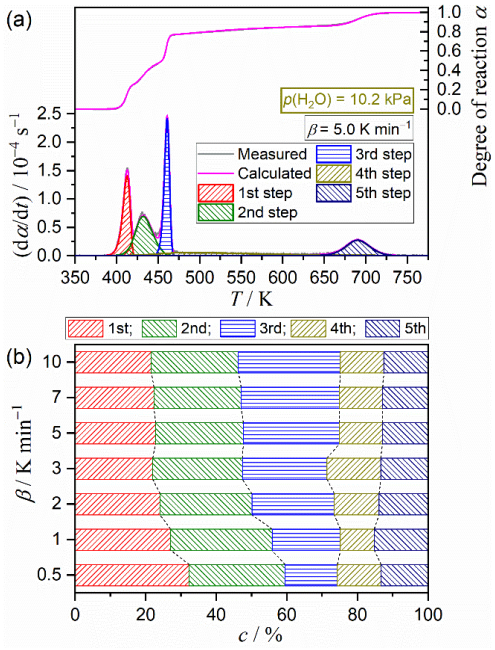

Figure S53. Results of KDA for the multistep thermal dehydration of DCPD (63–75 μm) in a stream of N_2–H_2O mixed gas with $p(H_2O)$ = 10.2 kPa: (a) typical fitting results for the overall reaction under linear nonisothermal conditions at a β of 5 K min^{-1} and (b) contributions of individual steps at various β values.

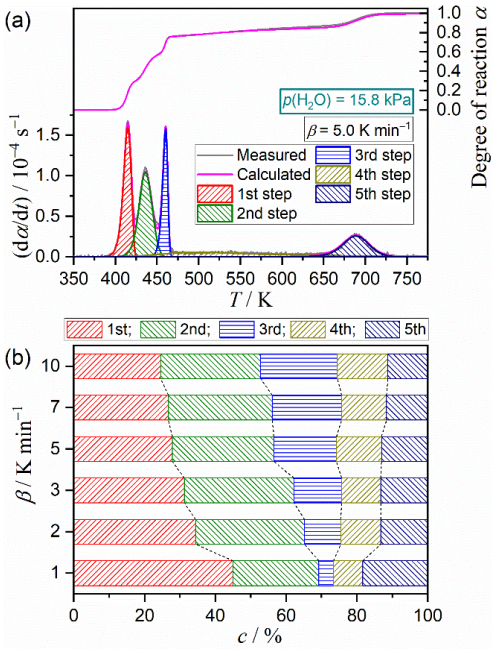

Figure S54. Results of KDA for the multistep thermal dehydration of DCPD (63–75 μm) in a stream of N_2–H_2O mixed gas with $p(H_2O)$ = 15.8 kPa: (a) typical fitting results for the overall reaction under linear nonisothermal conditions at a β of 5 K min^{-1} and (b) contributions of individual steps at various β values.

Table S12. Optimized kinetic parameters for each reaction step of the partially overlapping five-step mass loss process of the thermal dehydration of DCPD (63–75 μm) in a stream of N_2–H_2O mixed gas with $p(H_2O)$ = 1.2 kPa, averaged over different β values

i	c_i	$E_{a,i}$ / kJ mol^{-1}	A_i / s^{-1}	SB(m_i, n_i, p_i)			$R^{2,a}$
				m_i	n_i	p_i	
1		145.8 ± 0.3	(6.85 ± 0.02) × 10^{16}	−0.92 ± 0.03	1.42 ± 0.08	1.34 ± 0.03	0.9973 ± 0.0024
2	0.77 ± 0.02[b]	204.5 ± 2.7	(1.37 ± 0.04) × 10^{23}	1.13 ± 0.14	2.04 ± 0.11	−0.88 ± 0.08	
3		795.7 ± 0.5	(2.03 ± 0.07) × 10^{88}	−4.68 ± 0.19	2.78 ± 0.12	4.40 ± 0.28	
4	0.10 ± 0.03	146.7 ± 5.6	(2.25 ± 0.01) × 10^{14}	21.7 ± 0.27	−3.24 ± 0.07	−21.9 ± 0.63	
5	0.14 ± 0.03	267.0 ± 0.6	(7.68 ± 0.08) × 10^{17}	2.44 ± 0.09	0.44 ± 0.05	−2.58 ± 0.13	

[a] Determination coefficient of the nonlinear least-squares analysis of the KDA.
[b] $c_1 + c_2 + c_3$.

Table S13. Optimized kinetic parameters for each reaction step of the partially overlapping five-step mass loss process of the thermal dehydration of DCPD (63–75 μm) in a stream of N_2–H_2O mixed gas with $p(H_2O)$ = 2.9 kPa, averaged over different β values

i	c_i	$E_{a,i}$ / kJ mol^{-1}	A_i / s^{-1}	SB(m_i, n_i, p_i)			$R^{2,a}$
				m_i	n_i	p_i	
1		155.2 ± 0.5	(9.07 ± 0.40) × 10^{17}	−1.03 ± 0.07	1.33 ± 0.11	1.46 ± 0.05	0.9973 ± 0.0025
2	0.74 ± 0.02[b]	199.6 ± 1.9	(1.40 ± 0.01) × 10^{23}	5.06 ± 0.16	0.58 ± 0.01	−4.51 ± 0.08	
3		795.7 ± 0.4	(2.18 ± 0.03) × 10^{88}	−3.73 ± 0.10	2.44 ± 0.19	3.56 ± 0.11	
4	0.12 ± 0.02	143.4 ± 8.9	(2.22 ± 0.04) × 10^{14}	22.3 ± 0.54	−3.27 ± 0.03	−22.0 ± 0.34	
5	0.14 ± 0.01	277.4 ± 1.0	(5.71 ± 0.01) × 10^{18}	2.97 ± 0.08	0.33 ± 0.01	−2.94 ± 0.08	

[a] Determination coefficient of the nonlinear least-squares analysis of the KDA.
[b] $c_1 + c_2 + c_3$.

Table S14. Optimized kinetic parameters for each reaction step of the partially overlapping five-step mass loss process of the thermal dehydration of DCPD (63–75 μm) in a stream of N_2–H_2O mixed gas with $p(H_2O)$ = 6.3 kPa, averaged over different β values

i	c_i	$E_{a,i}$ / kJ mol^{-1}	A_i / s^{-1}	SB(m_i, n_i, p_i)			$R^{2,a}$
				m_i	n_i	p_i	
1		177.6 ± 0.6	(4.98 ± 0.61) × 10^{20}	−0.99 ± 0.13	1.19 ± 0.05	1.37 ± 0.13	0.9970 ± 0.0042
2	0.74 ± 0.03[b]	240.6 ± 2.1	(5.36 ± 0.16) × 10^{27}	5.70 ± 0.13	0.20 ± 0.01	−5.41 ± 0.17	
3		800.5 ± 0.6	(9.42 ± 0.88) × 10^{88}	−2.65 ± 0.28	2.09 ± 0.14	2.57 ± 0.35	
4	0.13 ± 0.04	144.4 ± 9.7	(4.13 ± 0.20) × 10^{14}	20.52 ± 1.32	−1.17 ± 2.31	−20.0 ± 1.57	
5	0.14 ± 0.02	253.9 ± 0.7	(1.25 ± 0.01) × 10^{17}	3.28 ± 0.29	0.37 ± 0.02	−3.00 ± 0.23	

[a] Determination coefficient of the nonlinear least-squares analysis of the KDA.
[b] $c_1 + c_2 + c_3$.

Table S15. Optimized kinetic parameters for each reaction step of the partially overlapping five-step mass loss process of the thermal dehydration of DCPD (63–75 μm) in a stream of N_2–H_2O mixed gas with $p(H_2O)$ = 8.1 kPa, averaged over different β values

i	c_i	$E_{a,i}$ / kJ mol^{-1}	A_i / s^{-1}	SB(m_i, n_i, p_i)			$R^{2,a}$
				m_i	n_i	p_i	
1		178.8 ± 2.9	(8.25 ± 5.00) × 10^{20}	−0.80 ± 0.02	1.18 ± 0.04	1.20 ± 0.03	0.9947 ± 0.0057
2	0.75 ± 0.02[b]	252.9 ± 0.6	(7.73 ± 0.03) × 10^{28}	4.93 ± 0.23	0.24 ± 0.01	−4.80 ± 0.22	
3		787.5 ± 0.5	(2.86 ± 0.03) × 10^{87}	−2.65 ± 0.08	1.90 ± 0.16	2.43 ± 0.08	
4	0.11 ± 0.02	156.2 ± 6.0	(4.26 ± 0.02) × 10^{14}	21.20 ± 0.13	−3.01 ± 0.01	−21.63 ± 0.21	
5	0.14 ± 0.01	239.1 ± 0.6	(8.96 ± 0.01) × 10^{15}	2.24 ± 0.03	0.63 ± 0.01	−1.93 ± 0.03	

[a] Determination coefficient of the nonlinear least-squares analysis of the KDA.
[b] $c_1 + c_2 + c_3$.

Table S16. Optimized kinetic parameters for each reaction step of the partially overlapping five-step mass loss process of the thermal dehydration of DCPD (63–75 μm) in a stream of N_2–H_2O mixed gas with $p(H_2O)$ = 10.2 kPa, averaged over different β values

i	c_i	$E_{a,i}$ / kJ mol^{-1}	A_i / s^{-1}	SB(m_i, n_i, p_i)			$R^{2,a}$
				m_i	n_i	p_i	
1		187.5 ± 0.3	(8.38 ± 0.42) × 10^{21}	−0.53 ± 0.02	1.16 ± 0.11	0.96 ± 0.02	0.9937 ± 0.0081
2	0.74 ± 0.02[b]	253.1 ± 0.4	(5.11 ± 0.01) × 10^{28}	4.43 ± 0.09	0.30 ± 0.01	−4.32 ± 0.19	
3		847.9 ± 0.5	(2.98 ± 0.03) × 10^{94}	−2.20 ± 0.07	1.88 ± 0.11	2.02 ± 0.17	
4	0.12 ± 0.02	161.2 ± 2.1	(4.28 ± 0.01) × 10^{14}	20.99 ± 0.16	−3.02 ± 0.02	−21.73 ± 0.16	
5	0.13 ± 0.01	244.7 ± 0.9	(2.63 ± 0.01) × 10^{16}	2.44 ± 0.05	0.62 ± 0.01	−2.14 ± 0.05	

[a] Determination coefficient of the nonlinear least-squares analysis of the KDA.
[b] $c_1 + c_2 + c_3$.

Table S17. Optimized kinetic parameters for each reaction step of the partially overlapping five-step mass loss process of the thermal dehydration of DCPD (63–75 μm) in a stream of N_2–H_2O mixed gas with $p(H_2O)$ = 15.8 kPa, averaged over different β values

i	c_i	$E_{a,i}$ / kJ mol^{-1}	A_i / s^{-1}	SB(m_i, n_i, p_i)			$R^{2,a}$
				m_i	n_i	p_i	
1		190.3 ± 0.4	(1.47 ± 0.12) × 10^{22}	−0.09 ± 0.01	1.13 ± 0.10	0.52 ± 0.04	0.9954 ± 0.0049
2	0.75 ± 0.01[b]	250.8 ± 0.4	(1.49 ± 0.05) × 10^{28}	2.22 ± 0.13	0.75 ± 0.05	−2.13 ± 0.10	
3		879.9 ± 0.6	(1.74 ± 0.16) × 10^{98}	−2.23 ± 0.13	1.89 ± 0.13	1.86 ± 0.11	
4	0.12 ± 0.03	164.2 ± 2.2	(4.23 ± 0.01) × 10^{14}	23.42 ± 0.72	−3.46 ± 0.05	−24.09 ± 0.50	
5	0.14 ± 0.03	243.8 ± 0.4	(2.51 ± 0.02) × 10^{16}	2.41 ± 0.06	0.60 ± 0.05	−2.08 ± 0.13	

[a] Determination coefficient of the nonlinear least-squares analysis of the KDA.
[b] $c_1 + c_2 + c_3$.

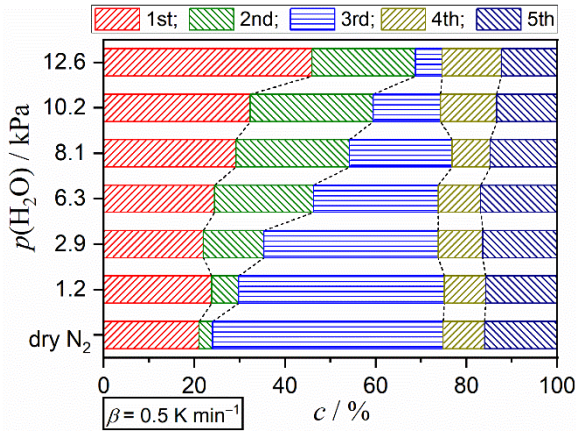

Figure S55. Variations in the contributions of component steps with $p(H_2O)$ value at a β of 0.5 K min^{-1}.

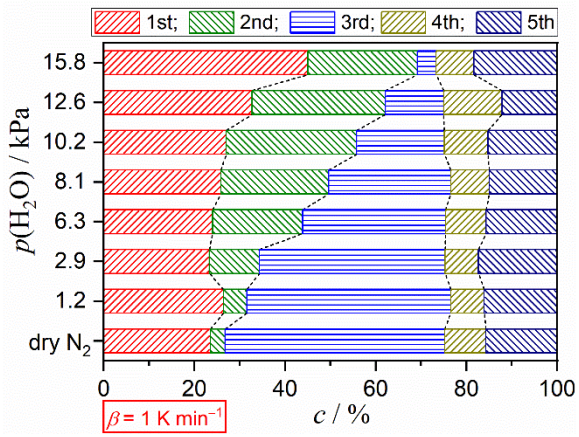

Figure S56. Variations in the contributions of component steps with $p(H_2O)$ value at a β of 1 K min^{-1}.

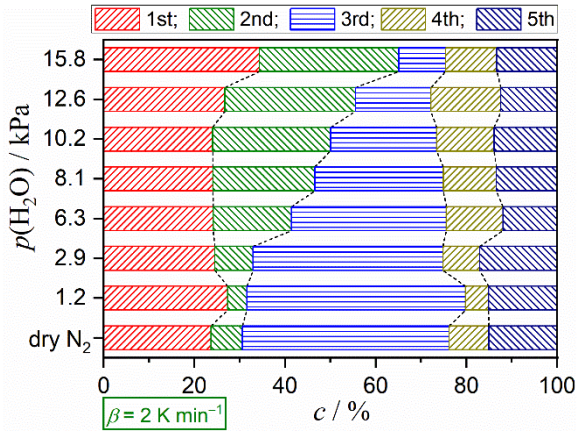

Figure S57. Variations in the contributions of component steps with $p(H_2O)$ value at a β of 2 K min^{-1}.

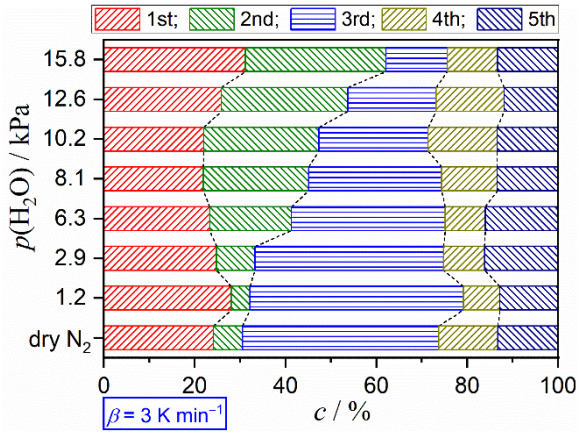

Figure S58. Variations in the contributions of component steps with $p(H_2O)$ value at a β of 3 K min^{-1}.

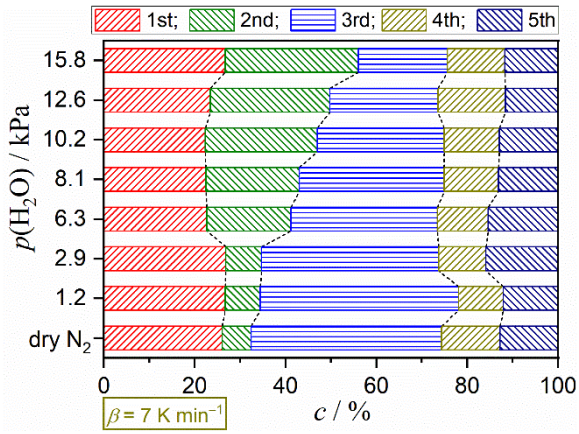

Figure S59. Variations in the contributions of component steps with $p(H_2O)$ value at a β of 7 K min^{-1}.

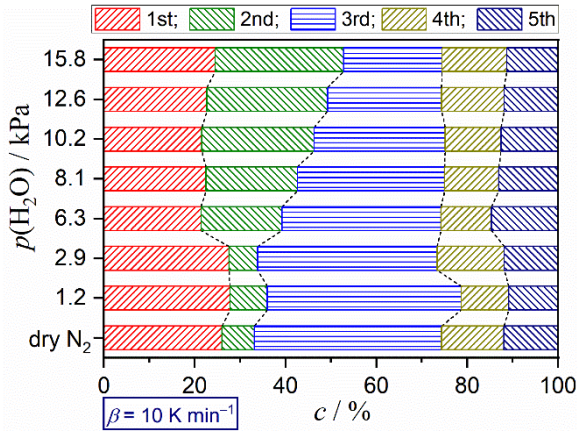

Figure S60. Variations in the contributions of component steps with $p(H_2O)$ value at a β of 10 K min^{-1}.

S5. Multistep Kinetics of the Thermal Dehydration of DCPA to form γ-CPP

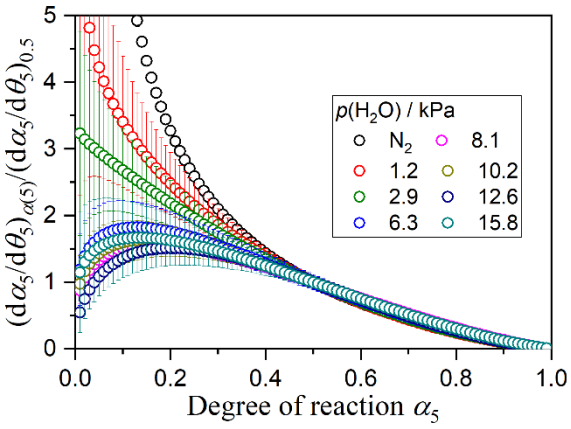

Figure S61. Normalized experimental master plots for the fifth mass loss step (the thermal dehydration of DCPA to form γ-CPP) at various atmospheric $p(H_2O)$ values.

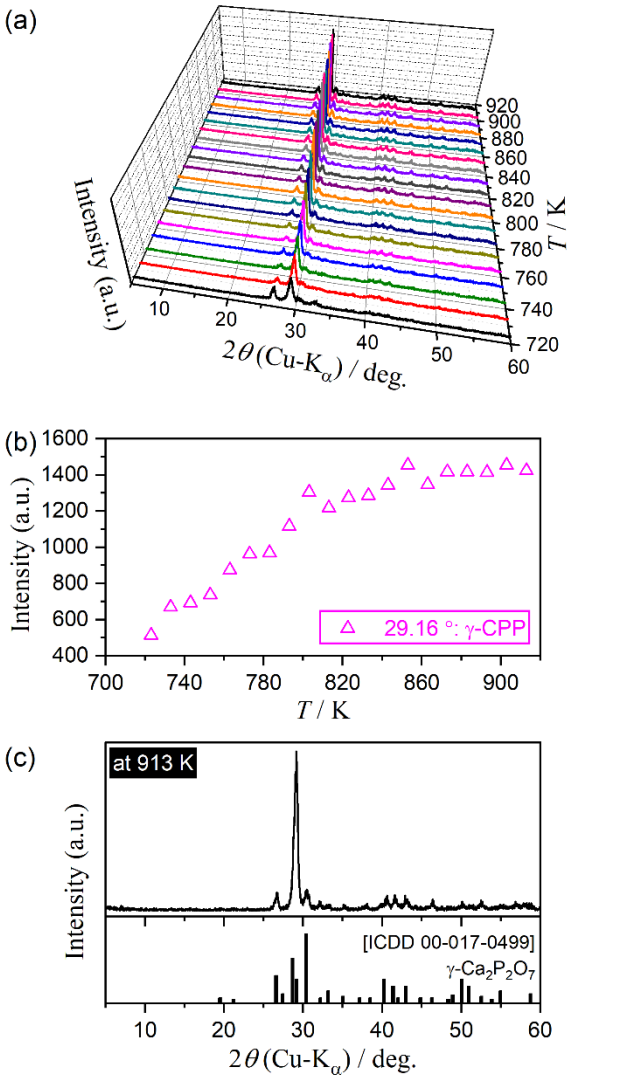

Figure S62. Change in the XRD pattern of DCPA during the stepwise isothermal heating in a stream of dry N_2 gas: (a) XRD patterns at different temperatures, (b) changes in the peak intensity of γ-CPP ($2\theta = 29.16°$), and (c) XRD pattern at 913 K.